

EPA-600/4-77-002b
February 1977

Environmental Monitoring Series

AN OBJECTIVE ANALYSIS TECHNIQUE FOR THE REGIONAL AIR POLLUTION STUDY Part II



**Environmental Sciences Research Laboratory
Office of Research and Development
U.S. Environmental Protection Agency
Research Triangle Park, North Carolina 27711**

RESEARCH REPORTING SERIES

Research reports of the Office of Research and Development, U.S. Environmental Protection Agency, have been grouped into five series. These five broad categories were established to facilitate further development and application of environmental technology. Elimination of traditional grouping was consciously planned to foster technology transfer and a maximum interface in related fields. The five series are:

1. Environmental Health Effects Research
2. Environmental Protection Technology
3. Ecological Research
4. Environmental Monitoring
5. Socioeconomic Environmental Studies

This report has been assigned to the ENVIRONMENTAL PROTECTION TECHNOLOGY series. This series describes research performed to develop and demonstrate instrumentation, equipment, and methodology to repair or prevent environmental degradation from point and non-point sources of pollution. This work provides the new or improved technology required for the control and treatment of pollution sources to meet environmental quality standards.

EPA-600/4-77-002b
February 1977

AN OBJECTIVE ANALYSIS TECHNIQUE
FOR THE REGIONAL AIR POLLUTION STUDY
PART II

by

D. Hovland
D. Dartt
K. Gage

Control Data Corporation
Minneapolis, MN 55440

68-02-1827

Project Officer

R. E. Eskridge
Meteorology and Assessment Division
Environmental Sciences Research Laboratory
Research Triangle Park, NC 27711

ENVIRONMENTAL SCIENCES RESEARCH LABORATORY
OFFICE OF RESEARCH AND DEVELOPMENT
U.S. ENVIRONMENTAL PROTECTION AGENCY
RESEARCH TRIANGLE PARK, NC 27711

DISCLAIMER

This report has been reviewed by the Environmental Science Research Laboratory, U. S. Environmental Protection Agency, and approved for publication. Approval does not signify that the contents necessarily reflect the views and policies of the U. S. Environmental Protection Agency, nor does mention of trade names or commercial products constitute endorsement or recommendation for use.

ABSTRACT

This report is concerned with the application of objective analysis techniques to the computation of trajectories from surface wind observations of the Regional Air Pollution Study in St. Louis. Trajectories were computed over a one hundred kilometer square grid centered on St. Louis for two five-hour periods during July 1975. The variability of the surface wind field was investigated by examination of the temporal and spatial variability of computed trajectories. Also, the sensitivity of the computed trajectories to the amount of data employed in the analysis was examined in some detail. The results showed a general lack of sensitivity of the computed trajectories to a single missing observation. However, computed trajectories were very sensitive to missing adjacent observations.

In addition to the trajectory analysis, a set of tapes containing gridded winds and temperatures for the St. Louis area were generated.

CONTENTS

Abstract	iii
Figures and Table,	vi
Abbreviations and Symbols	viii
1. Introduction	1
2. Conclusions and Recommendations	3
3. Objective Computation of Trajectories	4
4. Wind Trajectory Examples	9
5. Sensitivity of Computed Trajectories	27
References	37
Appendices	
A. Program Listings	38
B. Program Documentation	42
C. User Guide to Archive Tapes	44

FIGURES AND TABLE

<u>Number</u>		<u>Page</u>
1.	Diagram of trajectory computation	4
2.	Logical construction of the trajectory analysis program; overall construction	7
3.	Logical construction of the trajectory analysis program; detailed flow chart of trajectory displacement computation	8
4.	St. Louis RAMS observations on a square grid	10
5.	Hourly averaged surface winds for Day 197, 1975, plotted on the grid of Figure 4	11
6.	Hourly averaged surface winds for Day 210, 1975, plotted on the grid of Figure 4	12
7.	Trajectory starting points on the grid of Figure 4	13
8.	Inner trajectories for Day 197 on the grid of Figure 4	14
9.	Outer trajectories for Day 197 on the grid of Figure 4	15
10.	Inner trajectories for Day 210 on the grid of Figure 4	16
11.	Outer trajectories for Day 210 on the grid of Figure 4	17
12.	Spatial variability of air parcel vector displacements for trajectories of Day 197	19
13.	Spatial variability of air parcel vector displacements for trajectories of Day 210	20
14.	Temporal variability of the wind field for Day 197 as indicated by the scatter of trajectory end points for six individual hourly wind patterns; inner trajectories	22
15.	Temporal variability of the wind field for Day 197 as indicated by the scatter of trajectory end points for six individual hourly wind patterns; outer trajectories	23
16.	Temporal variability of the wind field for Day 210 as indicated by the scatter of trajectory end points for six individual hourly wind patterns; inner trajectories	25

FIGURES AND TABLE (continued)

<u>Number</u>		<u>Page</u>
17.	Temporal variability of the wind field for Day 210 as indicated by the scatter of trajectory end points for six individual hourly wind patterns; outer trajectories	26
18.	Departures of inner trajectory end points from reference values for Day 197 as the amount of data used in the analysis is varied. .	29
19.	Departures of outer trajectory end points from reference values for Day 197 as the amount of data used in the analysis is varied. .	30
20.	Departures of inner trajectory end points from reference values for Day 210 as the amount of data used in the analysis is varied. .	31
21.	Departures of outer trajectory end points from reference values for Day 210 as the amount of data used in the analysis is varied. .	32
22.	Dependence of the error, ϵ , in trajectory end points with the distance, Δ , of closest approach of the computed trajectory to the missing station for Day 197	34
23.	Dependence of the error, ϵ , in trajectory end points with the distance, Δ , of closest approach of the computed trajectory to the missing station for Day 210	35

TABLE

1.	Sequence of station combinations employed in the analysis leading to Figures 18, 19, 20, and 21	28
----	---	----

ABBREVIATIONS AND SYMBOLS

ABBREVIATIONS

RAMS -- Regional Air Monitoring System
RAPS -- Regional Air Pollution Study

SYMBOLS

r_i -- starting point of the i -th iteration in the computation of a trajectory
 t_i -- time associated with point r_i
 u_i -- west-east component of the wind at point r_i and time t_i
 v_i -- south-north component of the wind at point r_i and time t_i
 \vec{V}_i -- vector wind at point r_i and time t_i
 x_i -- west-east coordinate at point r_i
 y_i -- south-north coordinate at point r_i
 $(\Delta r)_i$ -- trajectory displacement associated with point r_i
 Δt -- time interval between iterations in trajectory computation
 $(\Delta x)_i$ -- west-east component of displacement $(\Delta r)_i$
 $(\Delta y)_i$ -- south-north component of displacement $(\Delta r)_i$
 ϵ -- trajectory end point displacement error
 Δ -- distance of closest approach of a trajectory to the location of a station with missing data.

SECTION 1

INTRODUCTION

The Regional Air Pollution Study (RAPS) was initiated in 1972 by the Environmental Protection Agency to collect the necessary data base for the development and verification of mathematical air quality models. The primary source of data for the RAPS program is a surface network of twenty-five automated meteorological and air quality monitoring stations located in St. Louis, MO. Data from this Regional Air Monitoring System (RAMS) are recorded routinely and checked for quality in St. Louis. The data used as input to the trajectory analysis described here are hourly averages of wind from all stations in the network. The surface data are supplemented by a less dense network of upper air soundings. Routinely, these consist of four rawinsonde soundings per day at each of two locations (one urban and one rural), plus pibal wind soundings at these same two locations every hour that rawinsonde ascents are not scheduled. These two upper air sounding stations are supplemented during intensive periods of data collection by an additional two stations operating on the same schedule.

An objective analysis program has been developed (Hovland, et al., 1976) to transform data at unequally spaced observation points to evenly spaced grid points. This program utilizes the scan weighting technique for the horizontal interpolation of observed data. Basically, this method is one of applying corrections to a first guess field where each observation provides a correction to the initial guess at each grid point lying within a circle of influence of an observation point. Successive corrections are then made to the field until reasonable consistency is realized between observations and computed values at the grid points.

This report is concerned with the application of the objective analysis program presented in Part 1 of this Final Report to the computation of trajectories. Only the surface data are used since the RAMS network

provides a much better defined wind field than can be obtained from only a few upper air soundings.

The technique for computing trajectories is presented in Section 3. Application of the trajectory analysis to the St. Louis data is presented in Section 4. An analysis of the sensitivity of computed trajectories to the amount of data included in the analysis is reported in Section 5. Appendices A and B contain program listings and documentation.

Appendix C contains documentation for a set of RAPS data archive tapes generated with the objective analysis program described above. The seven archive tapes contain gridded upper air winds and gridded surface winds and temperatures for the period 14 July through 15 August, 1975. These tapes are available at the Environmental Science Research Laboratory of the Environmental Protection Agency.

SECTION 2

CONCLUSIONS AND RECOMMENDATIONS

An objective technique for computing trajectories utilizing objectively analyzed wind fields has been developed and applied to surface winds observed during the Regional Air Pollution Study in St. Louis. The computed trajectories are not too sensitive to the amount of data included in the analysis provided the wind field is well sampled. The wind field is very well sampled in the center of the grid, where stations are less than ten kilometers apart. However, the wind is not as well sampled in the outer regions of the grid where a station may be as far as 30 km from its nearest neighbor. If it should happen that more than one of these outlying observations is missing, the wind field analysis may be seriously degraded and the trajectory computations will be in error. Every effort should be made to keep the key outermost observing stations in operation for the remainder of RAPS.

The sensitivity analysis reported here provides further evaluation of the objective analysis technique reported in Part 1 (Hovland, et al., 1976). The evaluation presented in Part 1 was based primarily on the appearance of contour patterns. Although contour patterns appear rather sensitive to the amount of data employed in the analysis, computed trajectories appear much less so. At least for the limited amount of data examined in this report the sensitivity analysis supports the conclusion that the wind field is sufficiently well sampled that computed trajectories are not significantly degraded when data from any single station are lost. The results of the analysis also inspire confidence in the adequacy of the objective analysis technique reported in Part 1.

SECTION 3

OBJECTIVE COMPUTATION OF TRAJECTORIES

The objective computation of trajectories requires a time sequence of gridded wind fields. A program to transform unequally spaced wind observations to a regular grid has been described earlier in Part 1 (Hovland, et al., 1976). Trajectories computed for this report use surface wind fields objectively analyzed by this technique. Wind observations are from a month of RAMS data (14 July through 15 August, 1975). The computed trajectories are confined to a horizontal plane to which all surface wind data have been assigned.

A trajectory is generated as a series of short line segments such as those in Figure 1 which run from point r_i to r_{i+1} and from r_{i+1} to r_{i+2} .

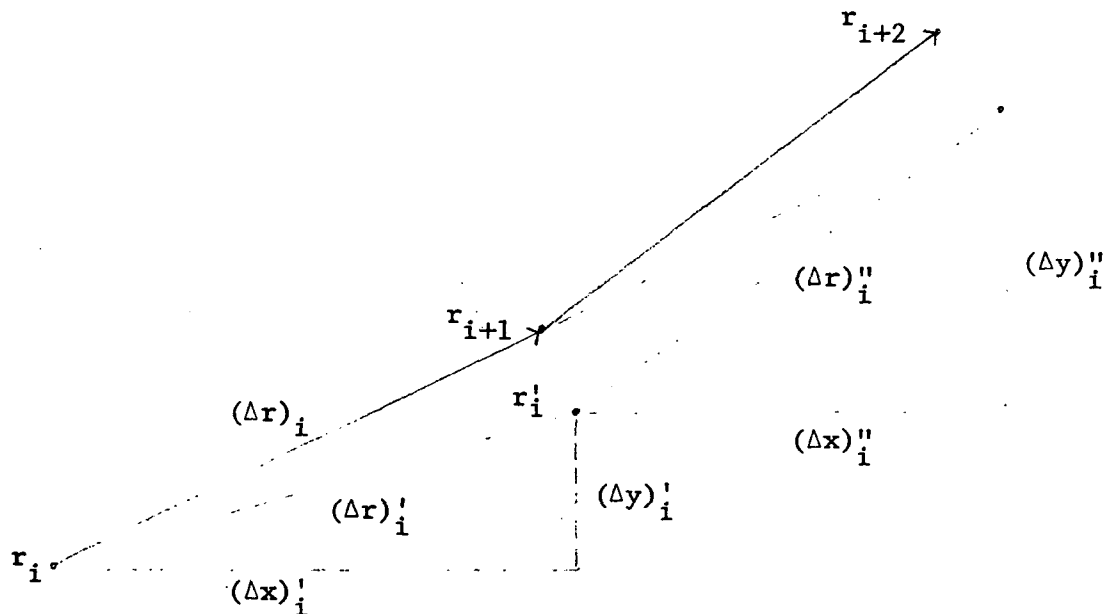


Figure 1. Diagram of trajectory computation. The trajectory displacement $(\Delta r)_i$ is the average of displacements $(\Delta r)'_i$ and $(\Delta r)''_i$.

A point, r_i , on the trajectory is defined by a west-east coordinate, x_i , and a south-north coordinate, y_i :

$$r_i = (x_i, y_i) \quad (1)$$

Associated with each point r_i is a time

$$t_i = t_0 + i\Delta t \quad (2)$$

The initial time, t_0 , is the time of the first gridded wind field. The time step, Δt , is chosen smaller than the time interval between the gridded wind fields.

The wind at point r_i and time t_i is defined by a west-east component, u_i , and a south-north component, v_i :

$$\vec{V}_i = \vec{V}(r_i, t_i) = (u_i, v_i) \quad (3)$$

\vec{V}_i is interpolated from the gridded wind fields, since, in general, r_i is not a grid point and t_i is not the time of one of the wind fields. The three-dimensional (x, y, t) linear interpolation function is given in Appendix A which contains a listing of the complete trajectory program. This interpolation function is an extension of the two-dimensional linear interpolation function which is derived in Part 1 (Hovland, et al., 1976).

The wind changes in both time and space along a trajectory. Each short trajectory segment should be computed with the average wind along its path. Since the exact average wind cannot be known until the segment is defined, a two stage procedure is used to approximate each segment. The trajectory calculation can be made as exact as desired by using a sufficiently small time step Δt . A first displacement, $(\Delta r)_i'$, is computed using the interpolated wind \vec{V}_i :

$$(\Delta r)_i' = [(\Delta x)_i', (\Delta y)_i'] \quad (4)$$

$$\text{where } (\Delta x)_i' = u_i \Delta t \quad (5a)$$

$$\text{and } (\Delta y)_i' = v_i \Delta t \quad (5b)$$

The displaced location, r_i' , in Figure 1 is then

$$r_i' = r_i + (\Delta r)_i' \quad (6)$$

$$\text{i.e., } x_i' = x_i + (\Delta x)_i' \quad (7a)$$

$$\text{and } y_i' = y_i + (\Delta y)_i' \quad (7b)$$

If r_i' is outside the grid on which the wind field is defined, it is redefined to be the same as r_i .

The wind interpolated at the displaced location r_i' is

$$\vec{V}_i' = \vec{V}(r_i', t_i + \Delta t) = (u_i', v_i') \quad (8)$$

which is then used to compute a second displacement:

$$(\Delta r)_i'' = [(\Delta x)_i'', (\Delta y)_i''] \quad (9)$$

$$\text{where} \quad (\Delta x)_i'' = u_i' \Delta t \quad (10a)$$

$$\text{and} \quad (\Delta y)_i'' = v_i' \Delta t \quad (10b)$$

The displacement, $(\Delta r)_i$, in Figure 1 used to advance the trajectory is the average of the first and second displacements:

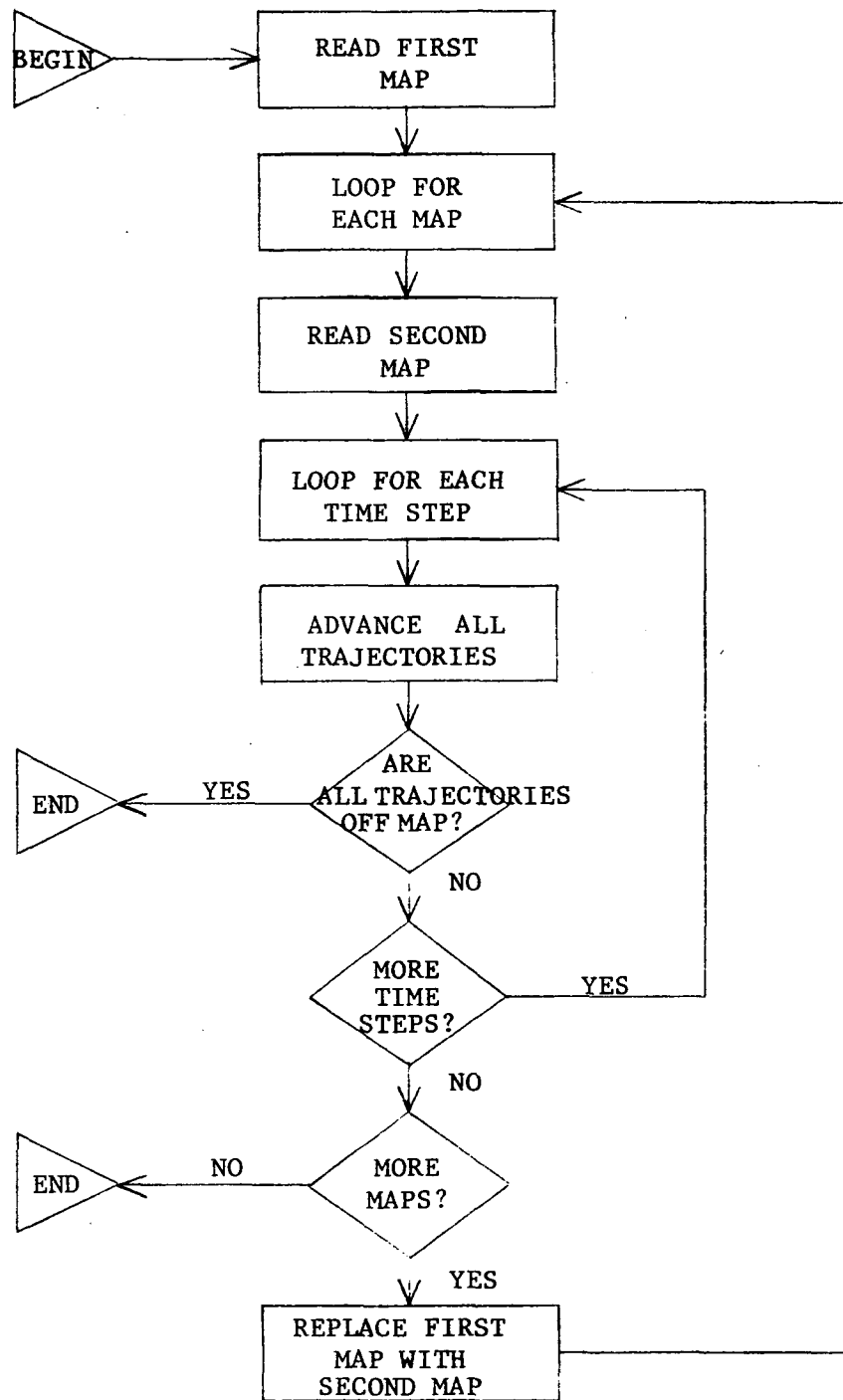
$$(\Delta r)_i = \left[\frac{(\Delta x)_i' + (\Delta x)_i''}{2}, \frac{(\Delta y)_i' + (\Delta y)_i''}{2} \right] \quad (11)$$

$$\text{then} \quad r_{i+1} = r_i + (\Delta r)_i \quad (12)$$

$$\text{and} \quad t_{i+1} = t_i + \Delta t = t_0 + (i+1)\Delta t \quad (13)$$

The above iterative procedure is repeated until point r_{i+1} is outside the grid or until t_{i+1} is greater than the time of the last gridded wind field.

The logical construction of the trajectory computation program is shown in Figures 2 and 3. In general, more than one trajectory will be generated but all trajectories must start at time t_0 (Equation 2). The time step, Δt , in the trajectory computation is adjustable. Tests have shown that trajectories computed from the hourly averaged RAMS data are not very sensitive to the magnitude of the time step, provided it is chosen to be less than one hour. All trajectories computed for this report have been generated with a time step of ten minutes.



COMPUTE: - SEVERAL TRAJECTORIES

- USING SEVERAL TIME STEPS BETWEEN MAPS

- USING SEVERAL MAPS

COMPUTATIONS ARE STOPPED IF ALL TRAJECTORIES ARE OFF THE MAP

Figure 2. Logical construction of the trajectory analysis program; overall construction.

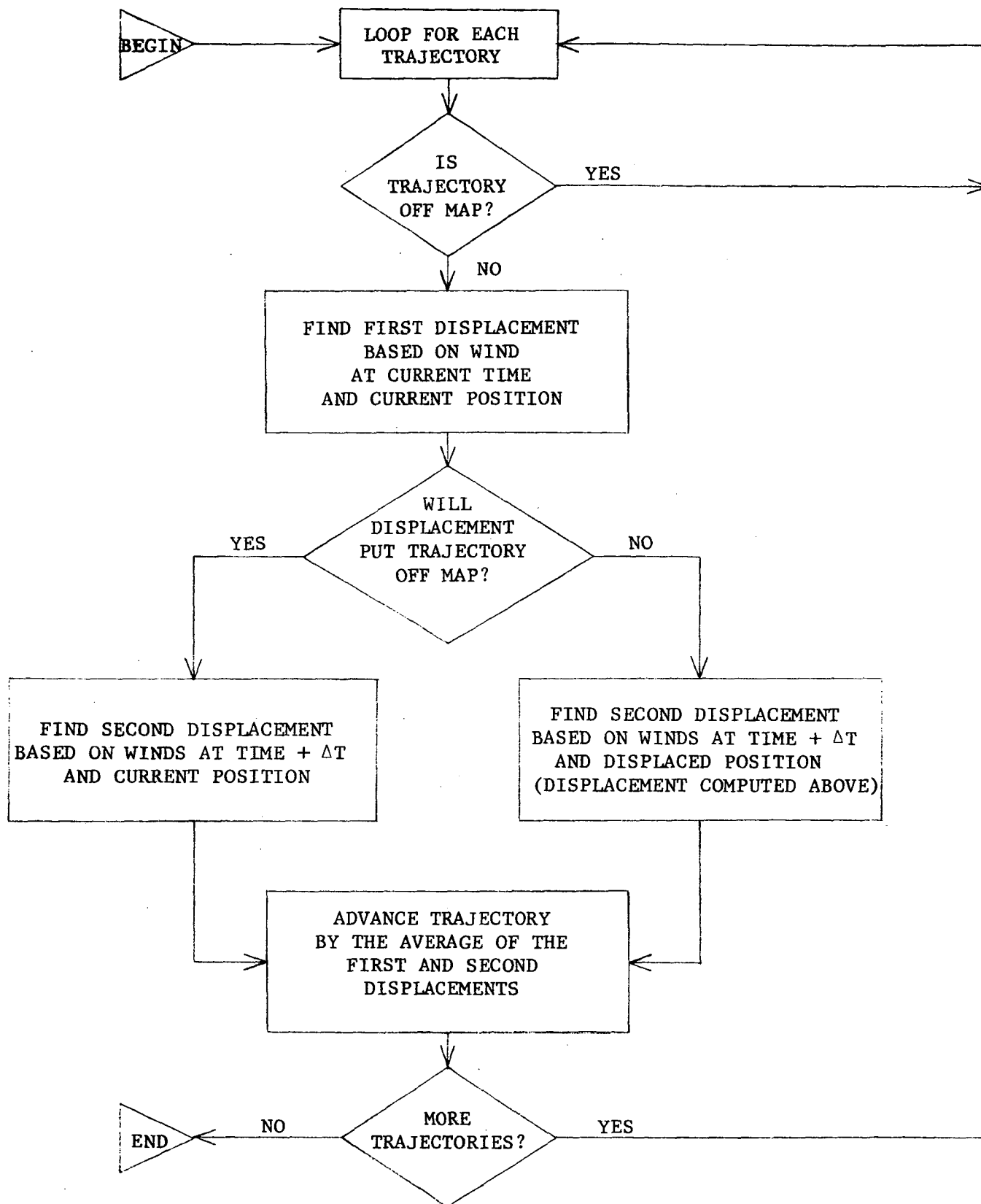


Figure 3.. Logical construction of the trajectory analysis program; detailed flow chart of trajectory displacement computation.

SECTION 4

WIND TRAJECTORY EXAMPLES

The St. Louis RAMS network of surface stations is shown in Figure 4. Also shown is the grid used for the objective analysis. Note that the density of stations decreases outward from the center of the city. As a result, smaller scale variability of winds can inherently be described near the center of the grid than at the external grid boundaries. Two five-hour periods have been chosen for detailed analysis of the trajectories and their sensitivity. Figure 5 shows the wind fields for the first period which is from Hour 00 to Hour 05 on Day 197, 1975. Figure 6 shows the wind fields for the second period which is from Hour 00 to Hour 05 on Day 210, 1975. On Day 197, data were missing from Stations 116, 120, and 124. On Day 210, data were missing from Stations 101, 109, 112, 119, 120 and 124. In addition, data from Station 102 were rejected for both days as unreliable. Thus, substantial fractions of the St. Louis grid are devoid of observations.

Two sets of trajectories were computed for each period. The trajectories had starting points as shown in Figure 7. Inner trajectories and outer trajectories computed for Day 197 are reproduced in Figures 8 and 9 respectively. For Day 210, inner and outer trajectories are shown in Figures 10 and 11. Trajectories can indicate convergence/divergence in the wind field if the area enclosed by a fixed distribution of trajectory starting points is greater/less than the area enclosed by the same respective distribution of trajectory end points. Figure 8 indicates a general convergence downwind of the central urban area during the five hour period of air passage on Day 197. The outer trajectories of Figure 9 indicate convergence in the southwest part of the grid but divergence in the eastern portion. The northern trajectories ③, ④ and ⑤ leave the grid during the five-hour period so they cannot be used to diagnose the wind convergence pattern. The flow patterns of Figure 5 illustrate the same basic pattern of convergence over the St. Louis grid as revealed by the trajectories. Here divergence is also indicated on the northern grid perimeter resulting from the increase in wind speed from about 2 to 4 meters/sec downwind of the urban area in the outer two rows of wind barbs. However, the

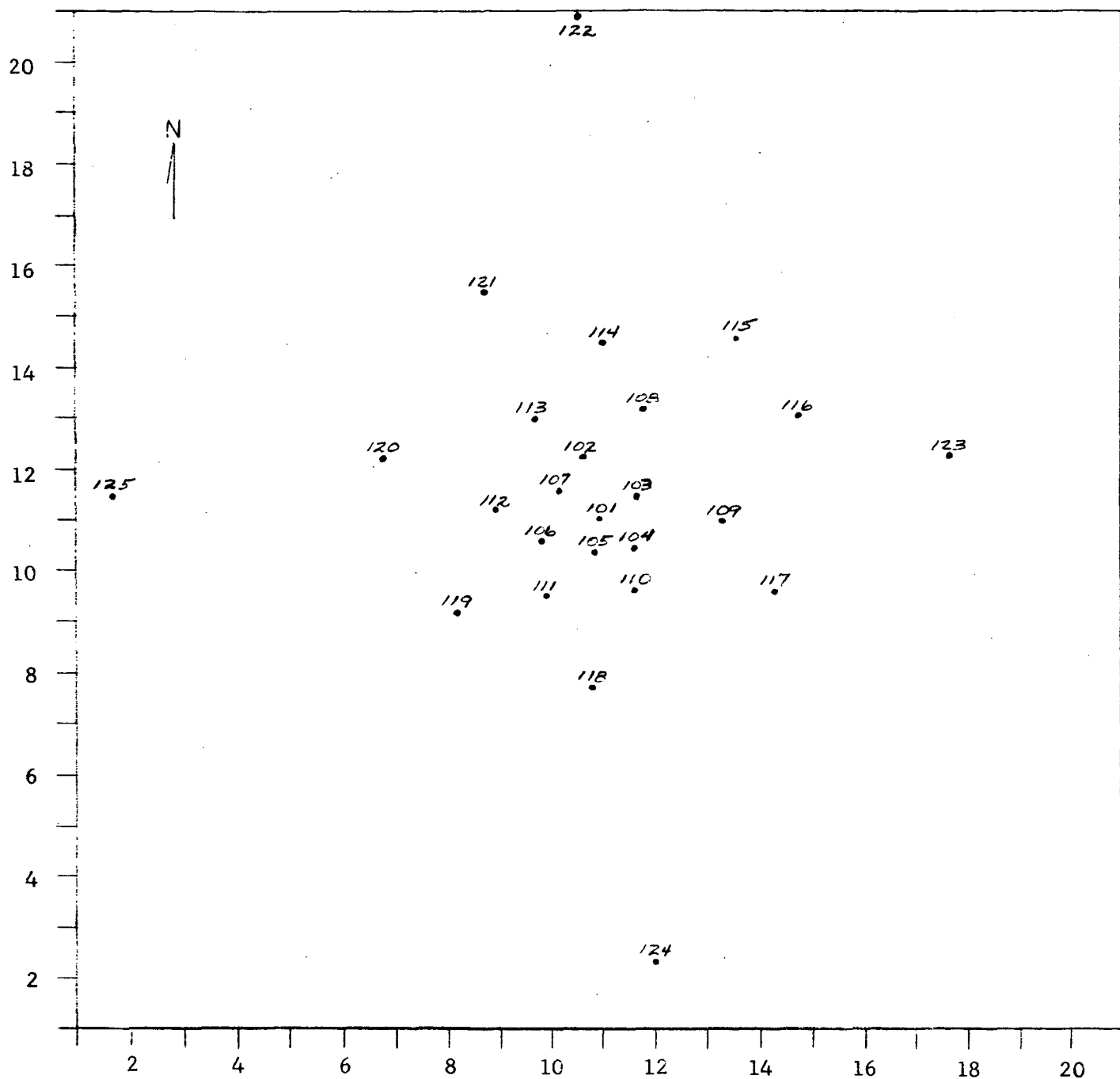
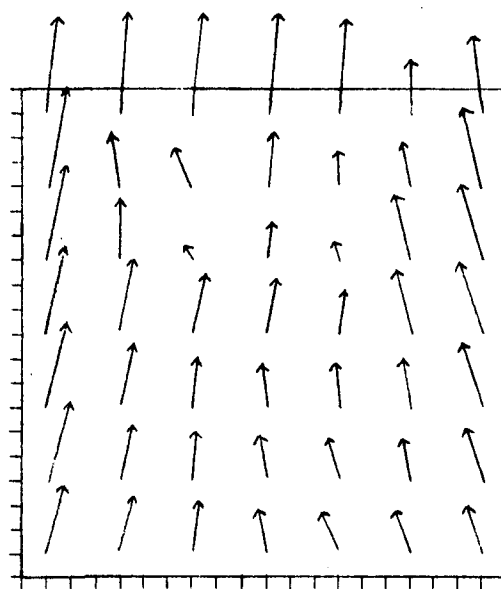
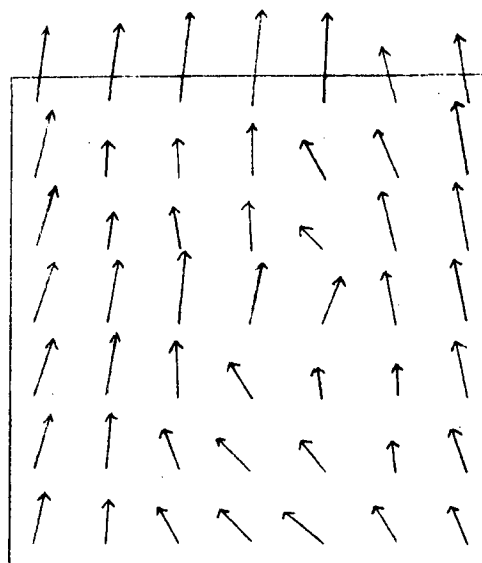


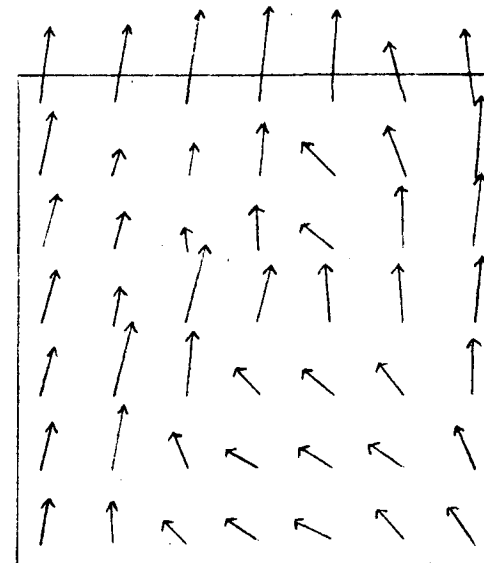
Figure 4. St. Louis RAMS stations on a square grid (grid interval = 5 km). The grid is positioned so that Station 101 is at the center point (11,11).



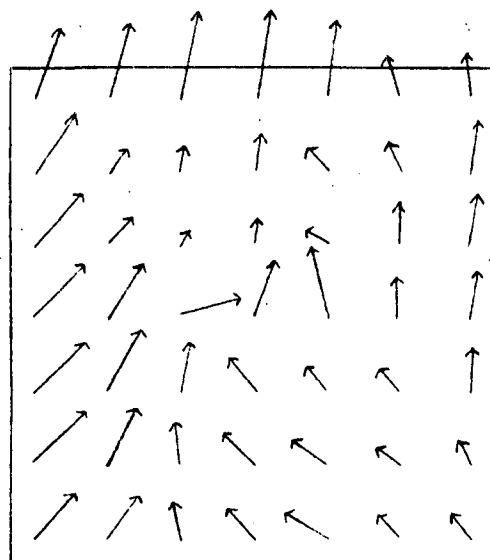
Hour 00



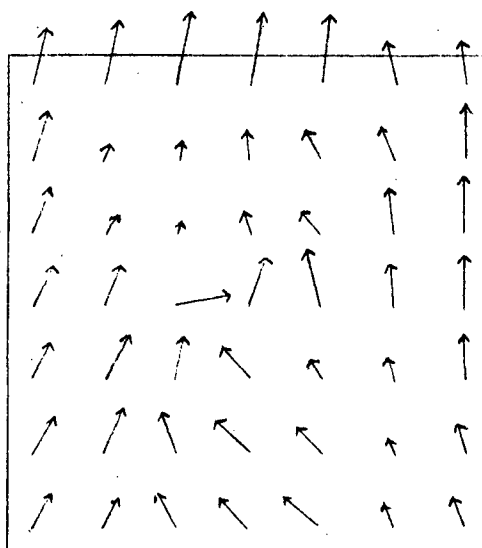
Hour 01



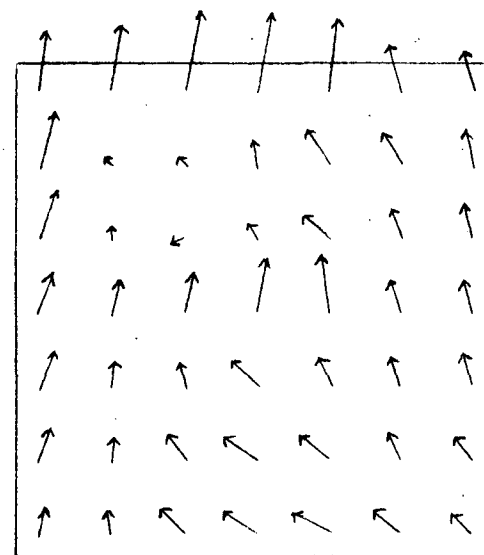
Hour 02




Hour 03

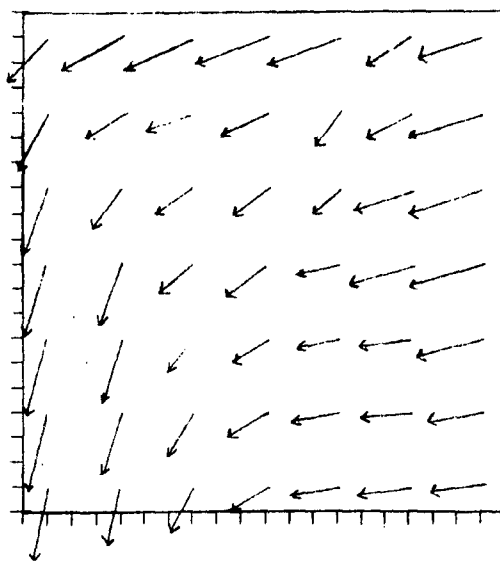


Hour 04

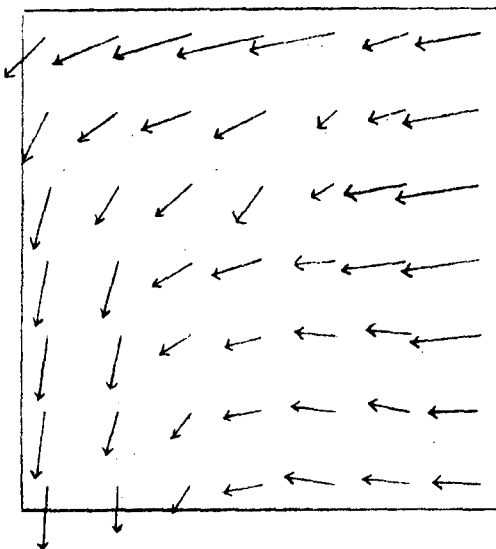


Hour 05

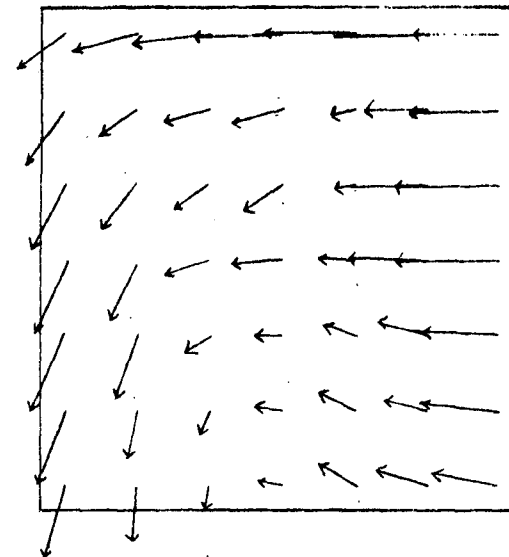
Figure 5. Hourly averaged surface winds for Day 197, 1975, Hours 00 to 05L, plotted on the grid of Figure 4. The length of each wind barb is proportional to the speed:  5 meters/sec.



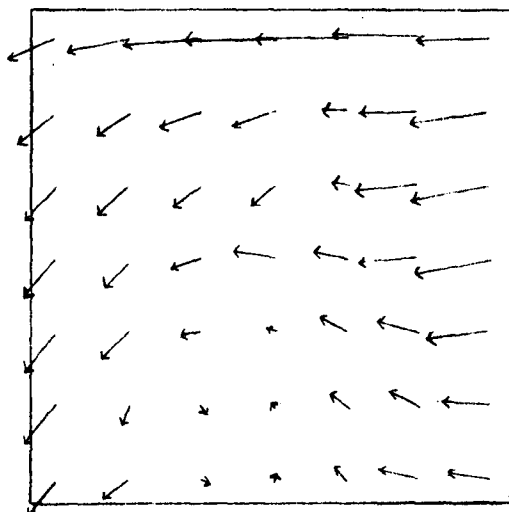
Hour 00



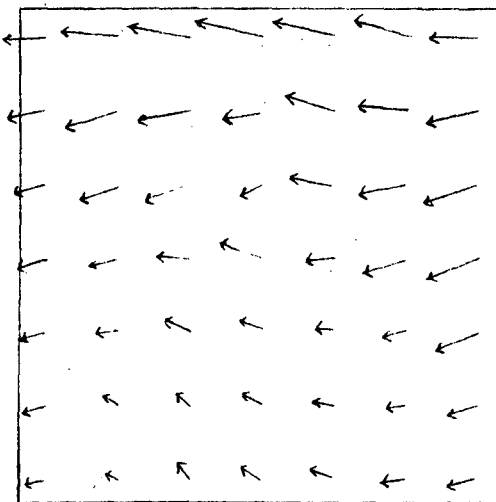
Hour 01



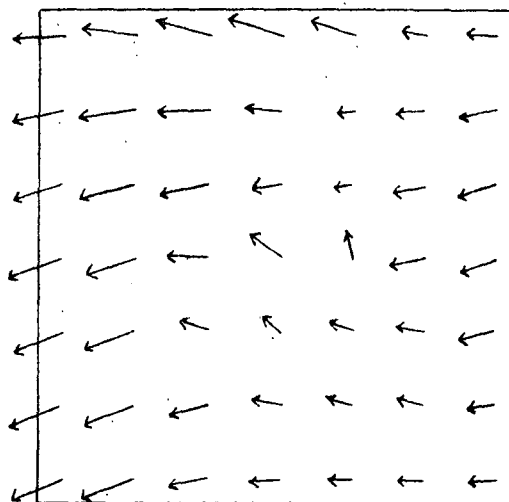
Hour 02




Hour 03



Hour 04



Hour 05

Figure 6. Hourly averaged surface winds for Day 210, 1975, Hours 00 to 05L, plotted on the grid of Figure 4. The length of each wind barb is proportional to the speed:  5meters/sec.

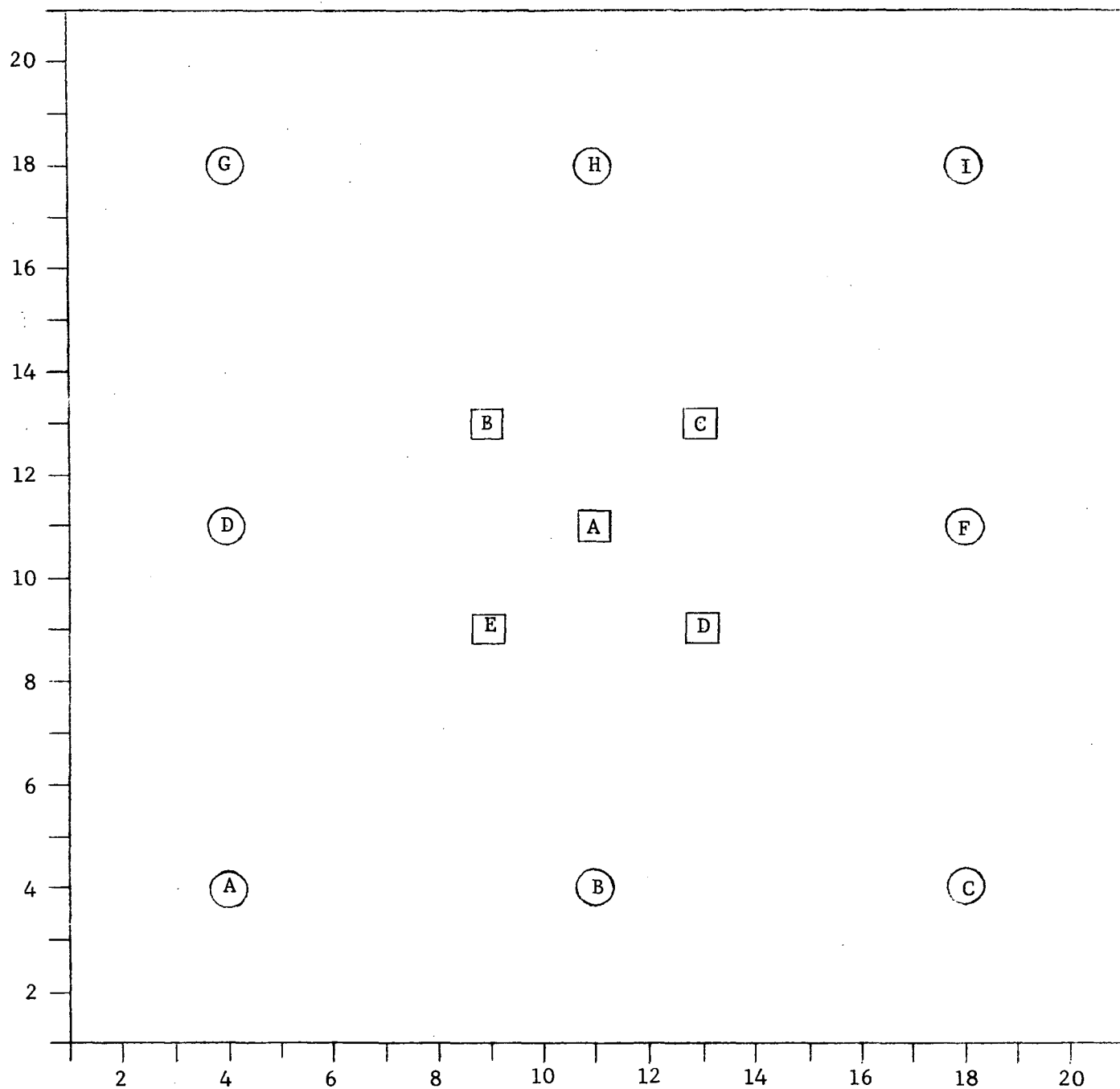


Figure 7. Trajectory starting points on the grid of Figure 4. Squares denote inner starting points; circles denote outer starting points. The starting point names are arbitrary; e.g., there is no connection between \textcircled{A} and \boxed{A} .

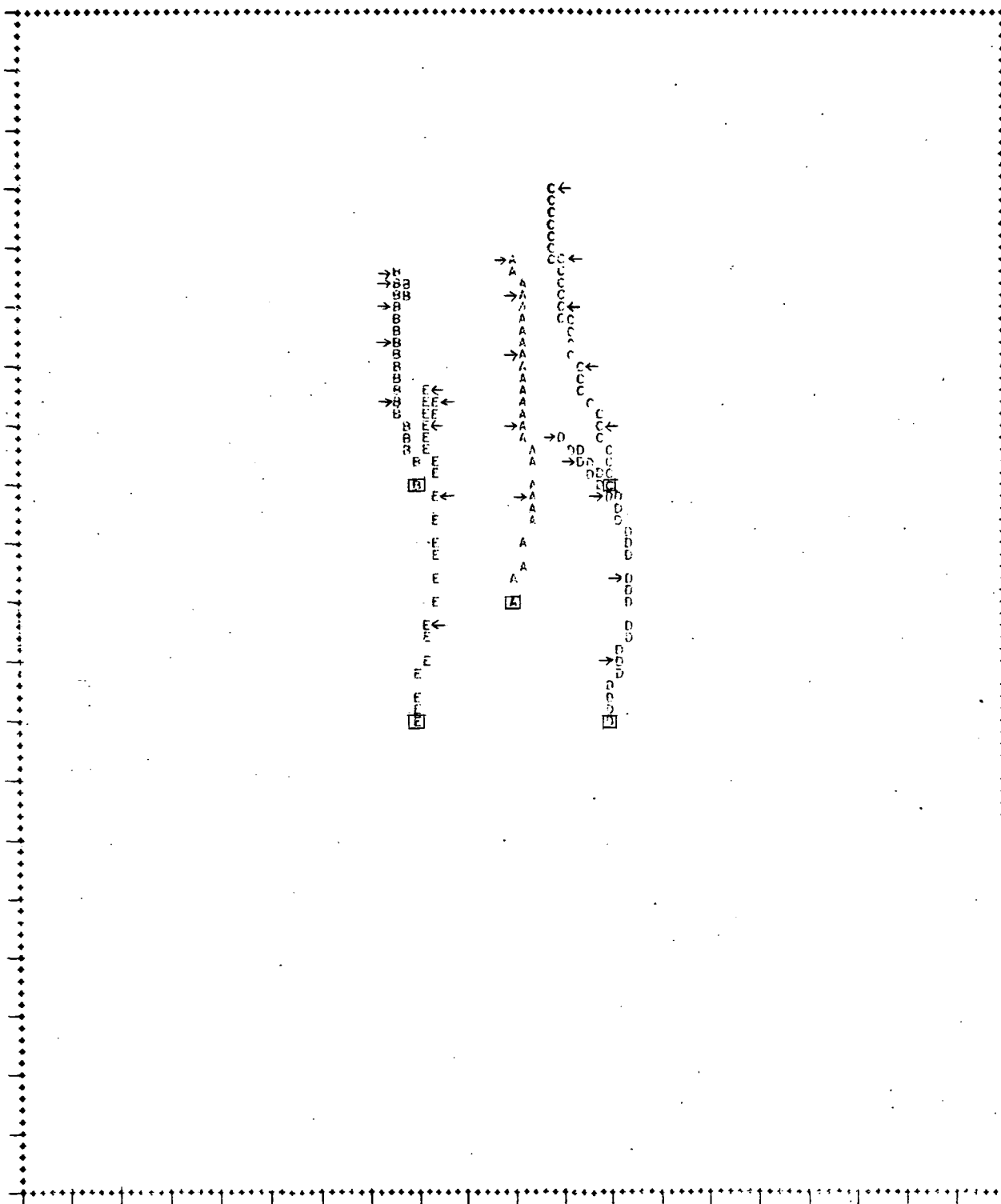


Figure 8. Inner trajectories for Day 197 on the grid of Figure 4. Arrows indicate positions after each hour.

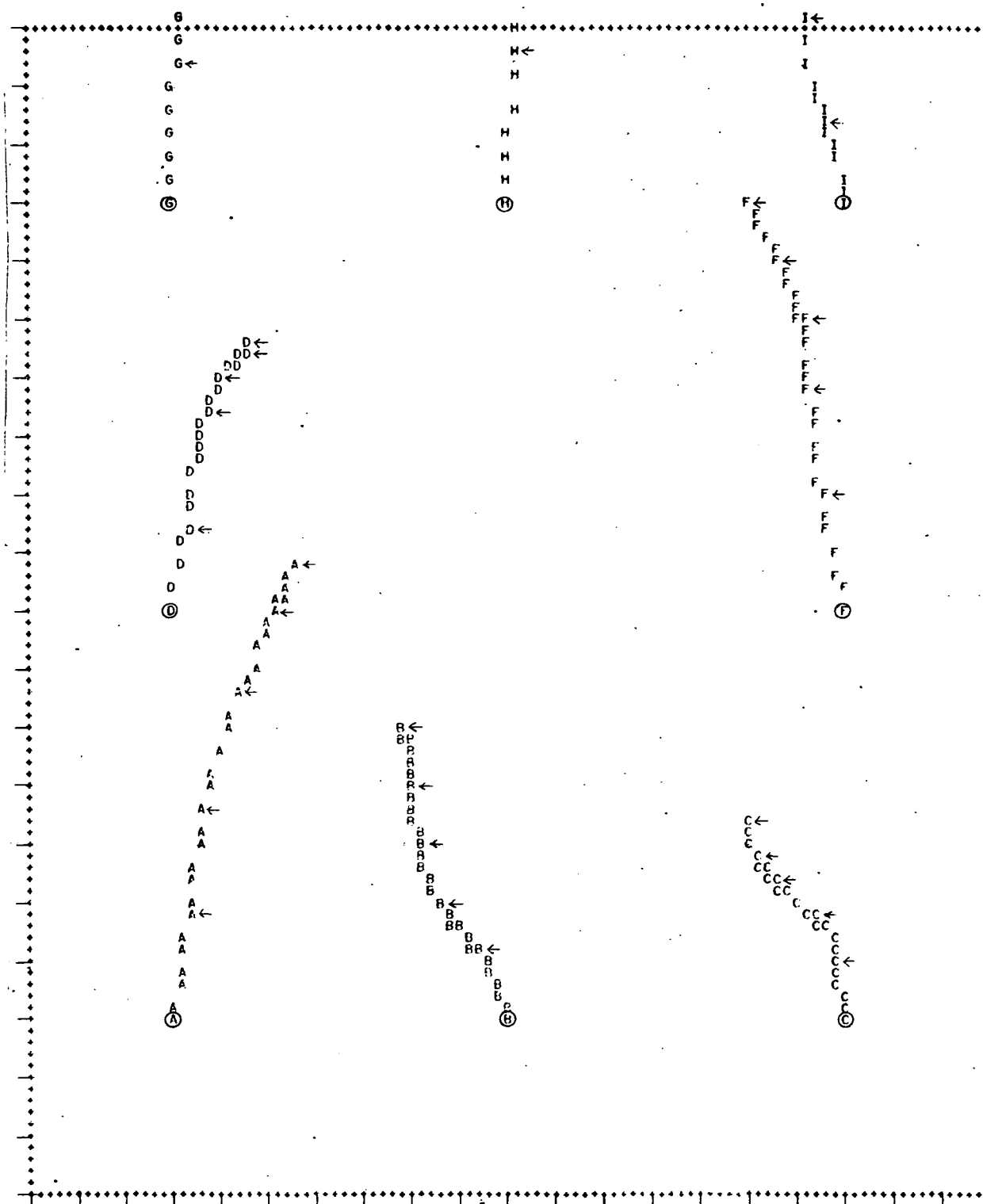


Figure 9. Outer trajectories for Day 197 on the grid of Figure 4. Arrows indicate positions after each hour.

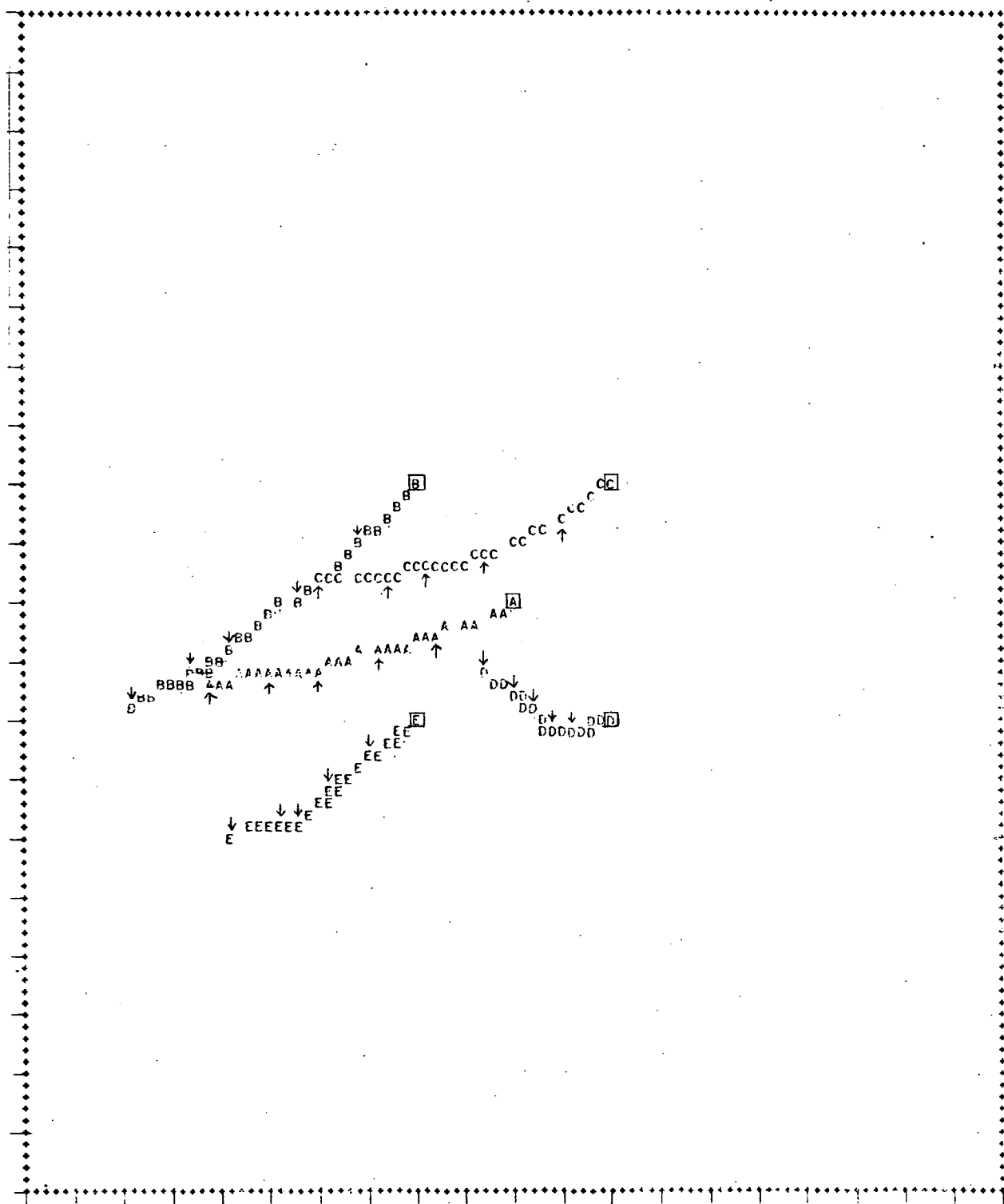


Figure 10. Inner trajectories for Day 210 on the grid of Figure 4. Arrows indicate positions after each hour.

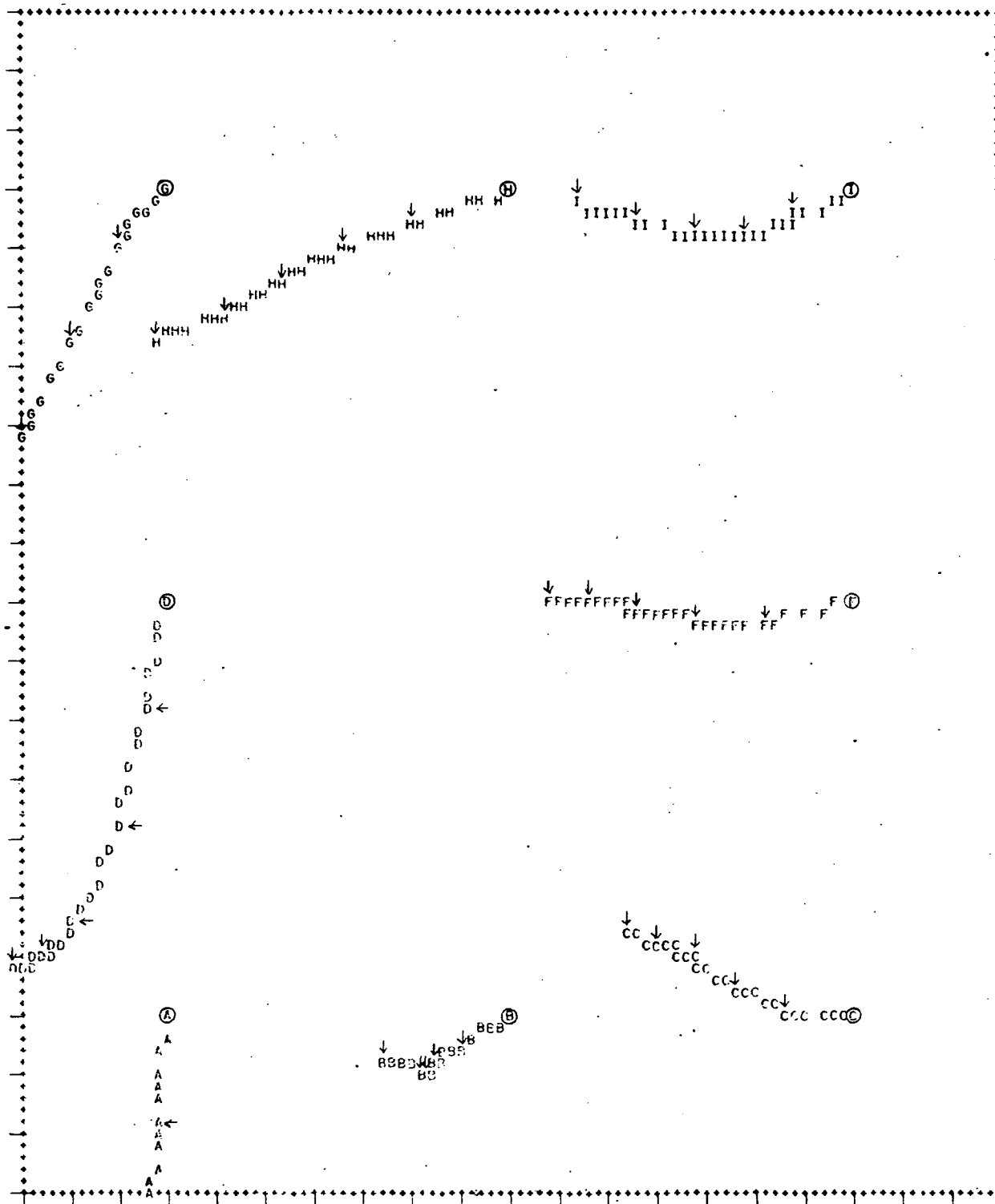


Figure 11. Outer trajectories for Day 210 on the grid of Figure 4. Arrows indicate positions after each hour.

perimeter grid winds in the current analysis are suspect because of a general lack of observations.

Figure 10 for Day 210 shows basically the same pattern of convergence downwind of the central urban area as on Day 197. The nocturnal flow patterns of Day 210, Figure 6, also exhibit cyclonic curvature of the wind at the center of the grid (city). Both downwind convergence and central cyclonic curvature with respect to urban St. Louis have recently been modeled theoretically by Vukovitch, et al., (1976) for light wind speed conditions. Cyclonic curvature is also evident on Day 197 surrounding the area of light winds which is displaced slightly downwind of the central urban area, Figure 5 (03, 04, 05L).

Besides indicating the movement of air parcels and the convergence pattern in the flow field, trajectories can also be used to reveal the space and time variability of wind within an area. A measure of the spatial variability of trajectories is revealed by the variation of the air parcel vector displacements (trajectory end point minus starting point) for various locations across the field. If the wind field were uniform, all air parcel displacements would be identical. The displacements for inner and outer starting points for Day 197 presented in Figure 12 are seen to vary greatly; indeed the variation is of the same magnitude as the displacements themselves. Also, the air parcel displacements for outer trajectory starting points tend to bracket the displacements for inner trajectory starting points.

Simulating the variability of air parcel displacements as a function of the density of input data is useful for estimating the actual trajectory errors for various distributions of observations. The variability in Figure 12, based on all available observations for Day 197, is thus a baseline measure of spatial variability for comparing sampling networks with fewer observations. In the extreme case, with a uniform wind field based on only one observation, the estimated trajectory error would be equivalent to the spatial variability (scatter) of displacements indicated on this diagram.

Note that trajectories started east of St. Louis (C, D, F) are displaced to the west, and trajectories started to the west of the city (B, E, D) are displaced more to the east. This pattern is consistent with convergence in the boundary layer over the city as discussed earlier. The corresponding air parcel displacements for Day 210 are reproduced in Figure 13. Again there

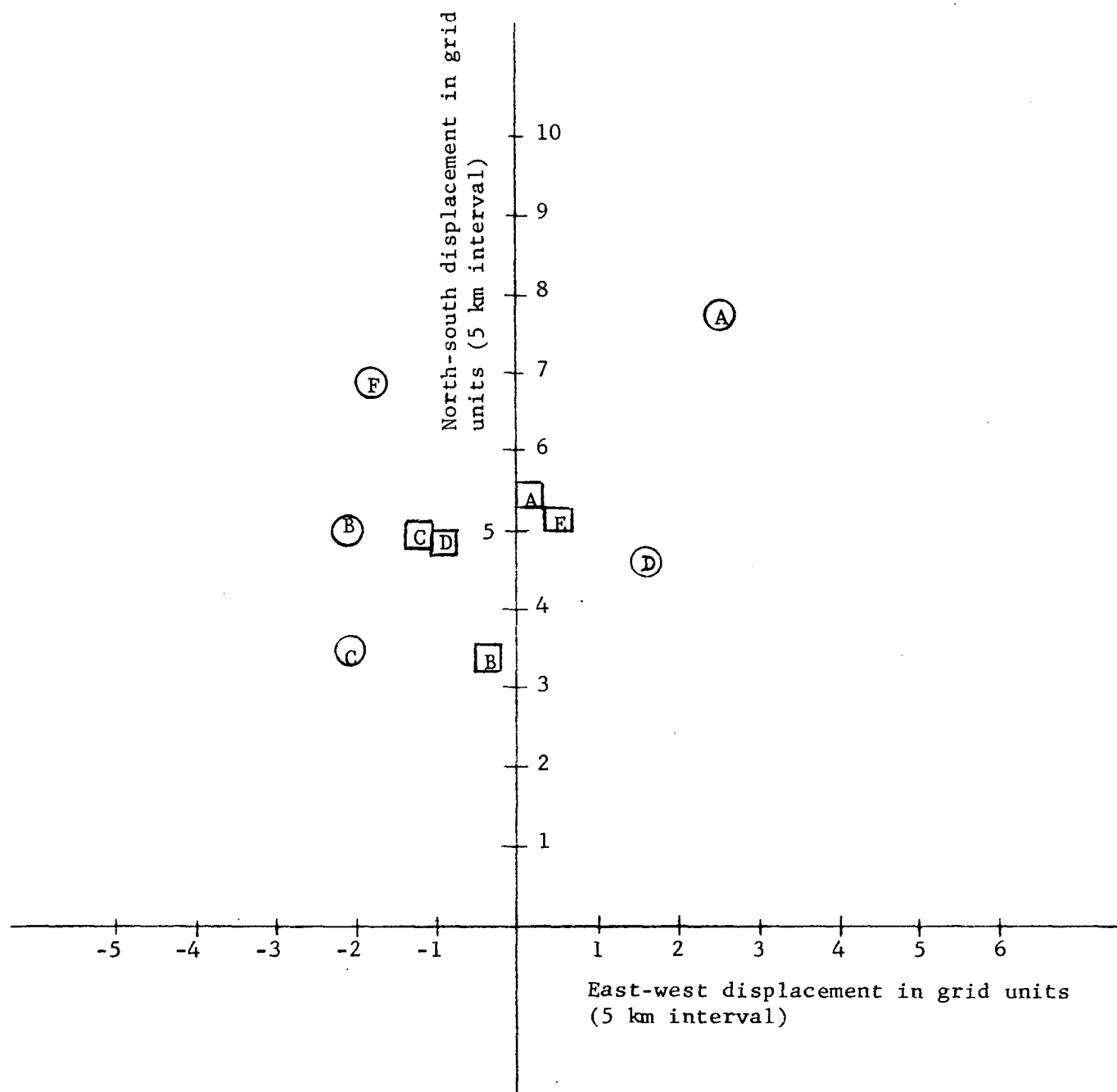


Figure 12. Spatial variability of air parcel vector displacements for trajectories of Day 197. The starting points of inner trajectories (\square) and outer trajectories (\circ) are shown in Figure 7.

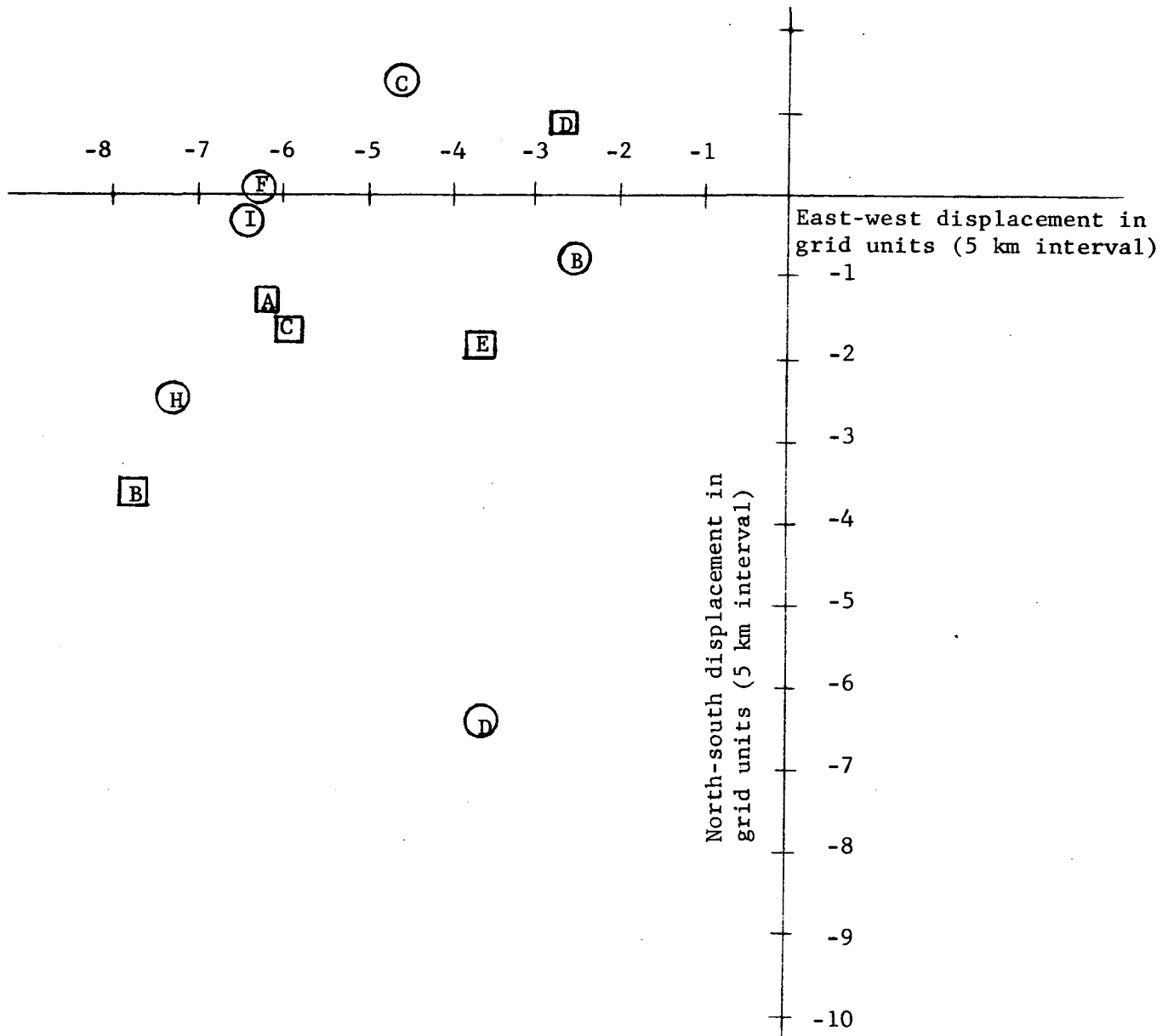


Figure 13. Spatial variability of air parcel vector displacements for trajectories of Day 210. The starting points of inner trajectories (\square) and outer trajectories (\circ) are shown in Figure 7.

appears to be some evidence for convergence in the urban boundary layer. For example, note that trajectories starting to the north of the city (E, C, H) are generally displaced further to the south than trajectories starting from south of the city (F, D, B).

The urban boundary layer convergence noted above is consistent with the circulation patterns expected due to the "heat island" effect. However, some of the observed variability is undoubtedly associated with the local topography. The influence of topography on the mesoscale wind field in a non-urban environment has been studied by Wendell (1972, 1975). Recently, Vukovich, *et al.*, (1976) have taken into account both the "heat island" effect and the influence of topography in a theoretical study of the St. Louis wind field. The results reported here seem consistent with circulation patterns deduced from the theoretical study.

One method of analyzing the time variation of the wind field is to analyze the variation of air parcel displacements from a fixed starting point as a function of chronologically observed wind patterns. Thus, each of the hourly wind patterns of Figure 5 is used to construct a separate vector displacement of five hours duration. The resulting six terminal points of these displacements for wind fields at 00, 01, 02, 03, 04, and 05L are then plotted on the St. Louis grid along with the end point of the conventional trajectory based on the time variation of winds throughout the five hour period (Figure 14). As the wind field changes from one hour to the next, the six trajectory end points based on the hourly wind patterns change. Only in the unlikely event that the wind field remains steady over the entire period will the end points be equal to one another and identical to the conventional trajectory end point.

Figure 14 (15) illustrates the trajectory end point analysis for the inner (outer) city trajectories of Figure 8 (9) for Day 197. The letters refer to the end points of the conventional trajectories whose starting points are given in Figure 7. The numbers 0-5 refer to trajectory end points generated with the analyzed wind fields of Hour 00 through Hour 05. The lines connect these end points based on hourly wind patterns with their corresponding conventional trajectory end points. The scatter of trajectory end points of the hourly wind patterns about a conventional trajectory end point is indicative of the temporal wind variability occurring in various portions of the field. Figures 16

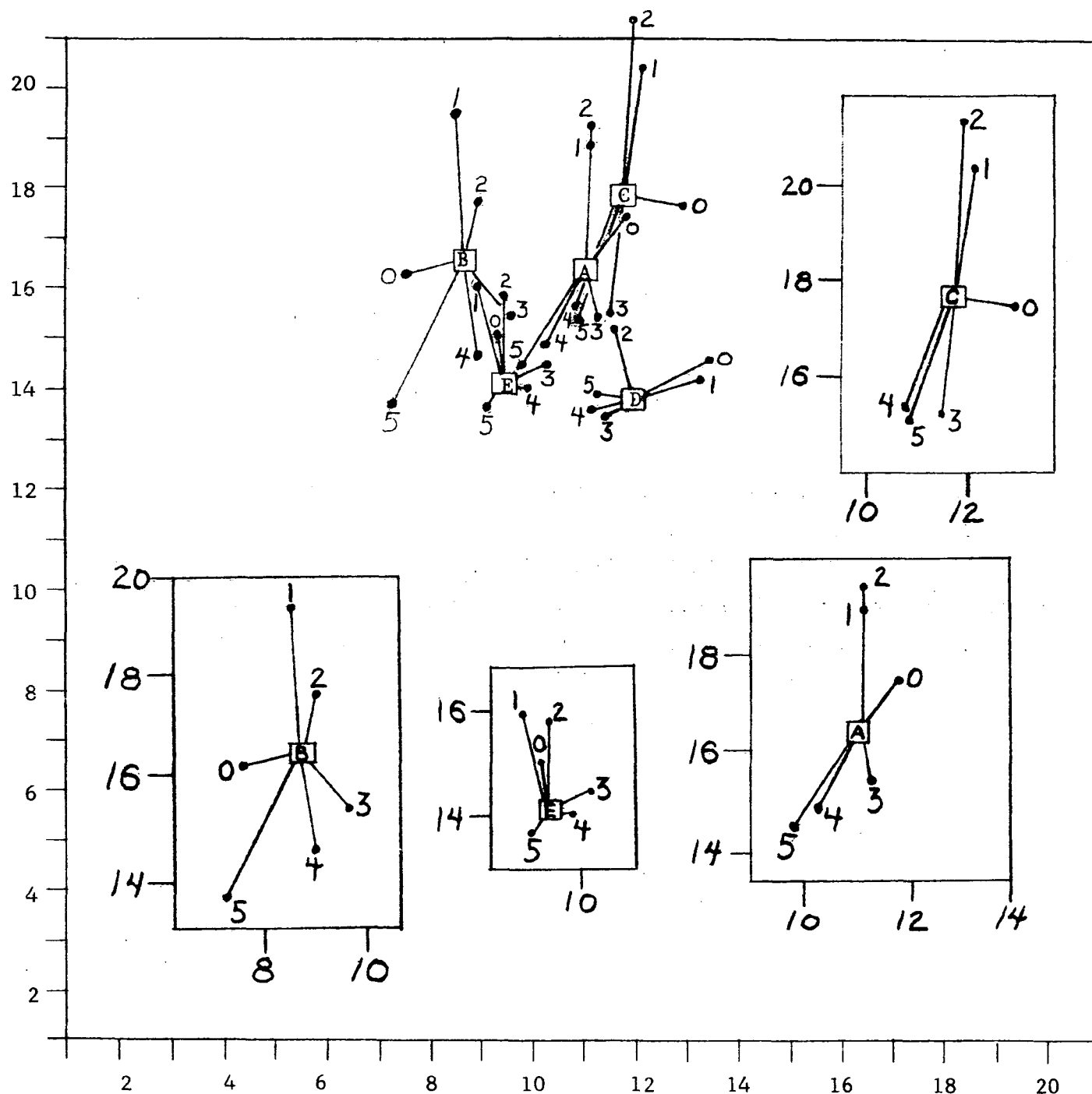


Figure 14. Temporal variability of the wind field for Day 197 as indicated by the scatter of trajectory end points for six individual hourly wind patterns (0, 1, 2, 3, 4, 5 local time). The letters indicate the location of the associated end points of the conventional inner trajectories of Figure 8 on the grid of Figure 4. Insets are used to show the temporal variability where the trajectory end points overlap. See text for further explanation.

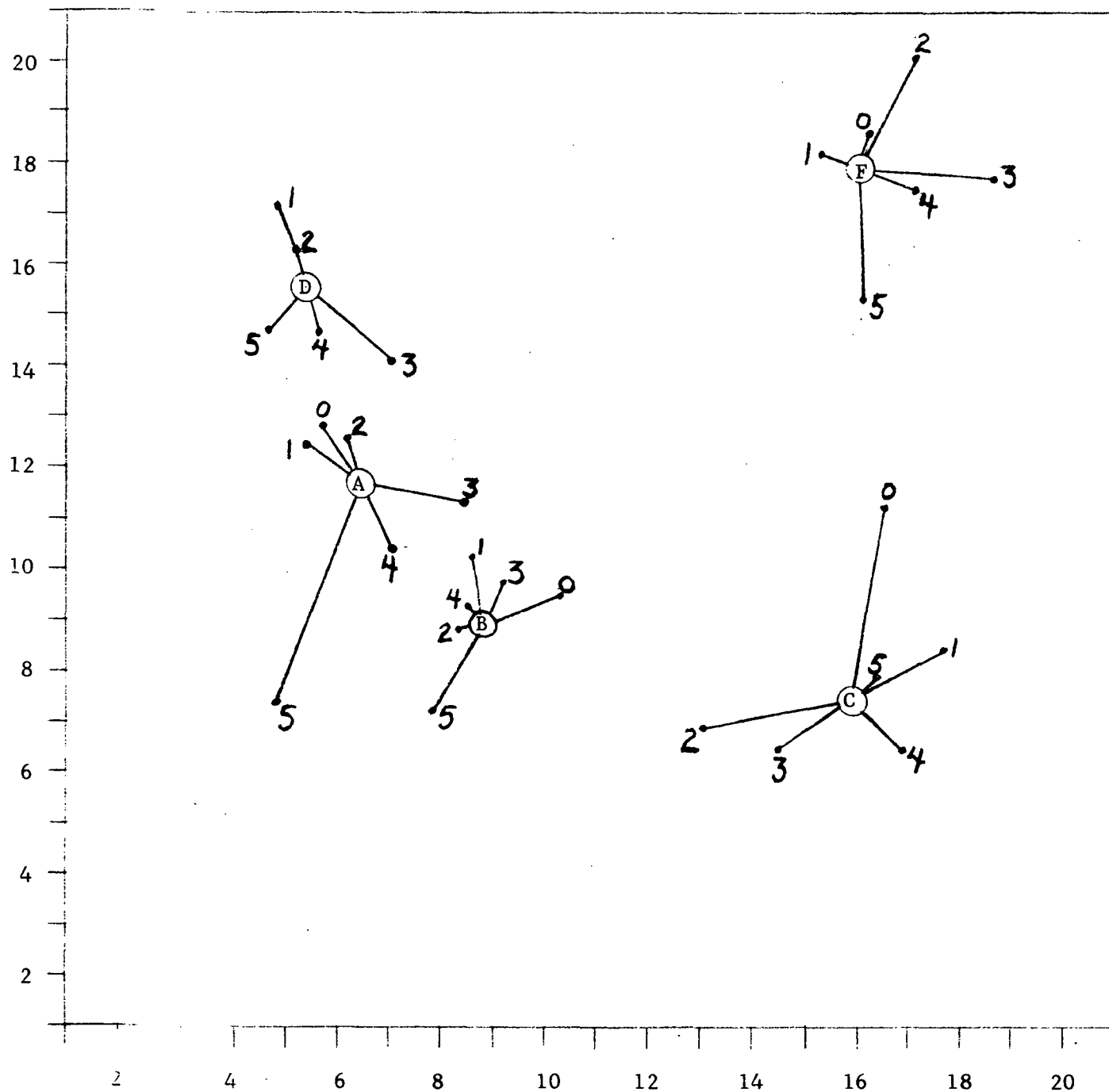


Figure 15. Temporal variability of the wind field for Day 197 as indicated by the scatter of trajectory end points for six individual hourly wind patterns (0, 1, 2, 3, 4, 5 local time). The letters indicate the location of the associated end points of the conventional outer trajectories of Figure 9 on the grid of Figure 4. See text for further explanation.

and 17 show that the time variability of winds on Day 210 is similar to that on Day 197. If the time variability of wind is accurately depicted by the spatial variability of trajectory end points as shown above, then the scatter of these end points about the end point of the conventional trajectory is representative of the error in trajectory displacement that would occur if observations were available only once within the five hour period. It is possible to simulate errors of trajectory displacement as a function of various distributions of observations in time as well as space.

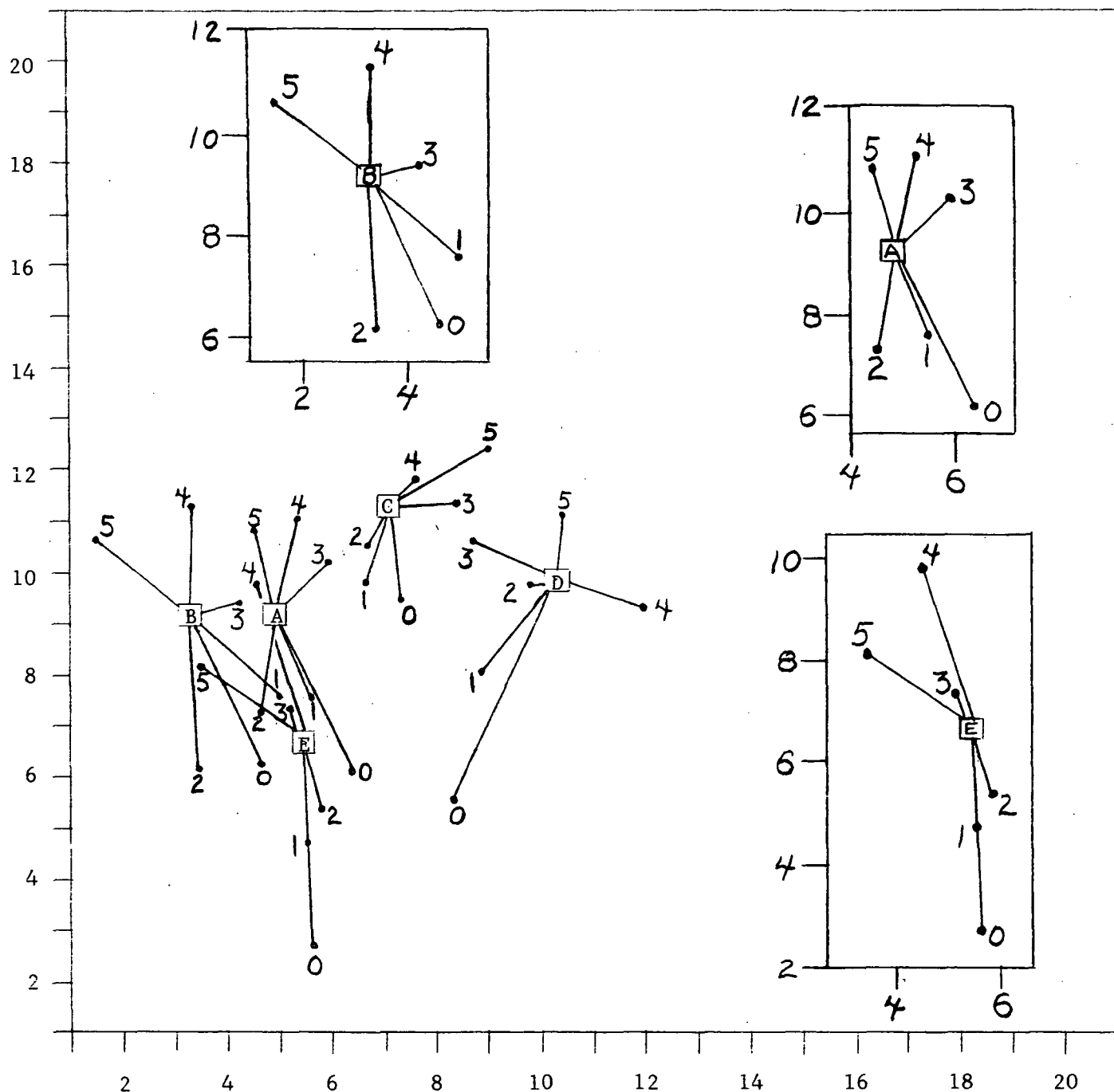


Figure 16. Temporal variability of the wind field for Day 210 as indicated by the scatter of trajectory end points for six individual hourly wind patterns (0, 1, 2, 3, 4, 5 local time). The letters indicate the location of the associated end points of the conventional inner trajectories of Figure 10 on the grid of Figure 4. Insets are used to show the temporal variability where the trajectory end points overlap. See text for further explanation.

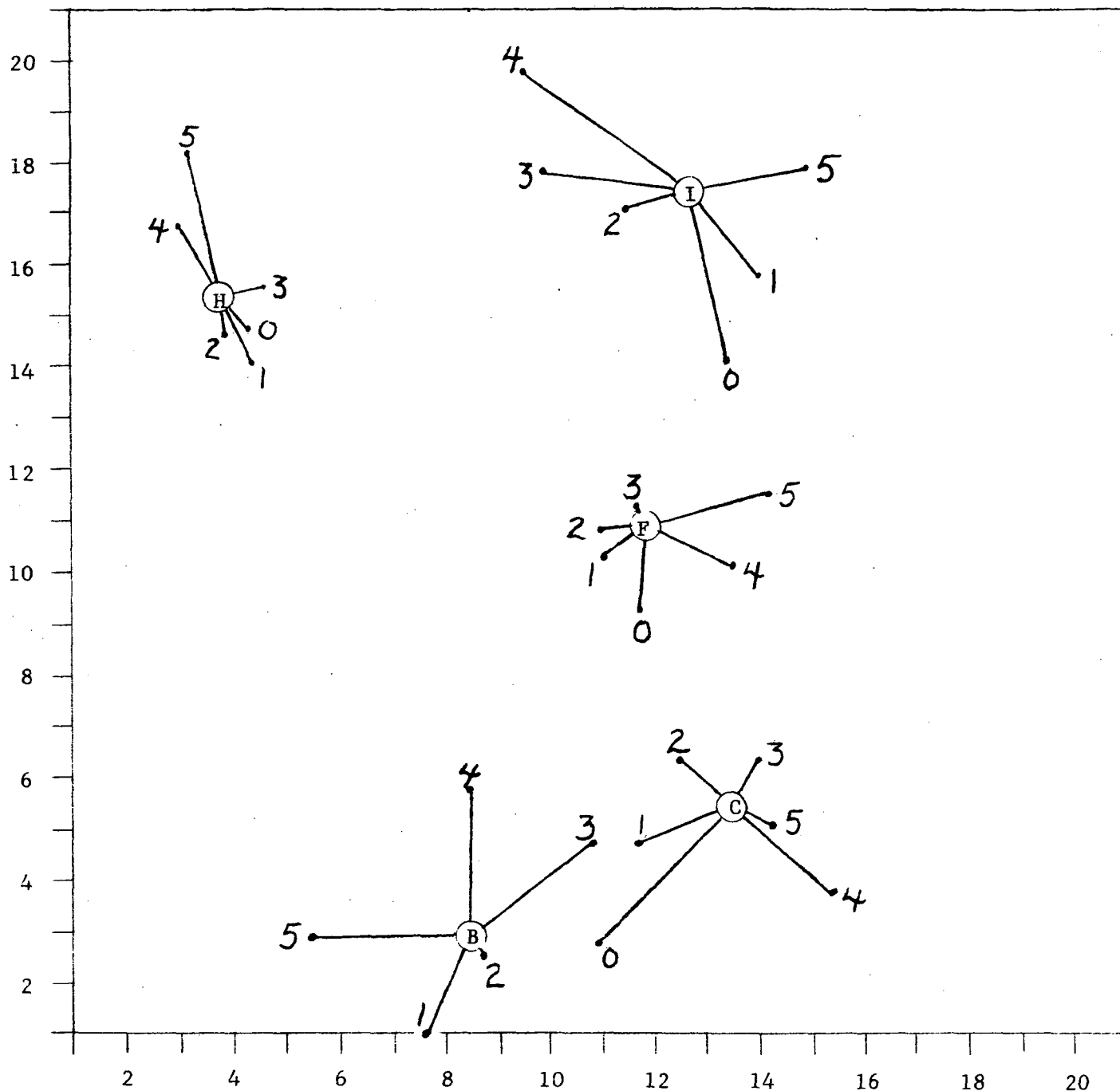


Figure 17. Temporal variability of the wind field for Day 210 as indicated by the scatter of trajectory end points for six individual hourly wind patterns (0, 1, 2, 3, 4, 5 local time). The letters indicate the location of the associated end points of the conventional outer trajectories of Figure 11 on the grid of Figure 4. See text for further explanation.

SECTION 5

SENSITIVITY OF COMPUTED TRAJECTORIES

Although trajectories can be generated without much difficulty, the degree to which the computed trajectories are representative of actual trajectories of material elements advected by the wind field will depend upon the quality of the analyzed wind fields. The quality of an analyzed wind field is dependent on the objective analysis technique, the accuracy of individual wind observations, and the adequacy of the observing network to resolve the variability of the field. One way to check the validity of computed trajectories would be to compare them with actual trajectories measured by tracking tetroons or tracers.

The approach followed here is to evaluate the sensitivity of analyzed trajectories to the amount of data employed in the analysis of the wind field. This sensitivity analysis should provide a good internal consistency check on the RAMS wind data and the objective analysis of the wind field.

The first test of the sensitivity of computed trajectories is to explore their convergence to the final trajectory as data are successively added to the wind field analysis starting with data from a single station and ending with all available data. The trajectory end points using all available data are used for reference. Trajectory end points computed using lesser amounts of data are compared to the reference values and their differences calculated. Table 1 lists the observations used for the sets of trajectories computed for the two days. For each trajectory, the vector differences in end point locations are plotted for all the data sets of Table 1. The results are reproduced in Figures 18, 19, 20, and 21. Figure 18 shows the inner trajectory end point differences for Day 197 and Figure 20 shows the inner trajectory end point differences for Day 210. These inner trajectory end points with a few exceptions converge to the final end points with the fifth data set. Although some cases can be found where adding more data actually displaces trajectory end points further from their final value, the general trend is for convergence toward the final value as more data are added.

TABLE 1.
SEQUENCE OF STATION COMBINATIONS EMPLOYED IN THE
ANALYSES LEADING TO FIGURES 18, 19, 20, AND 21

DATA SET	DAY 197	DAY 210
1	101	103
2	101, 122-125	103, 122 - 125
3	101, 114, 117, 119, 122-125	103, 116, 118-125
4	101, 114-125	103, 114-125
5	101, 108-125	103, 110-125
6	101, 104, 106, 108-125	103, 104, 106, 108-125
7	101-125	103-125
Missing from all data sets	102, 116, 120, 124	101, 102, 109, 112, 119, 120, 124

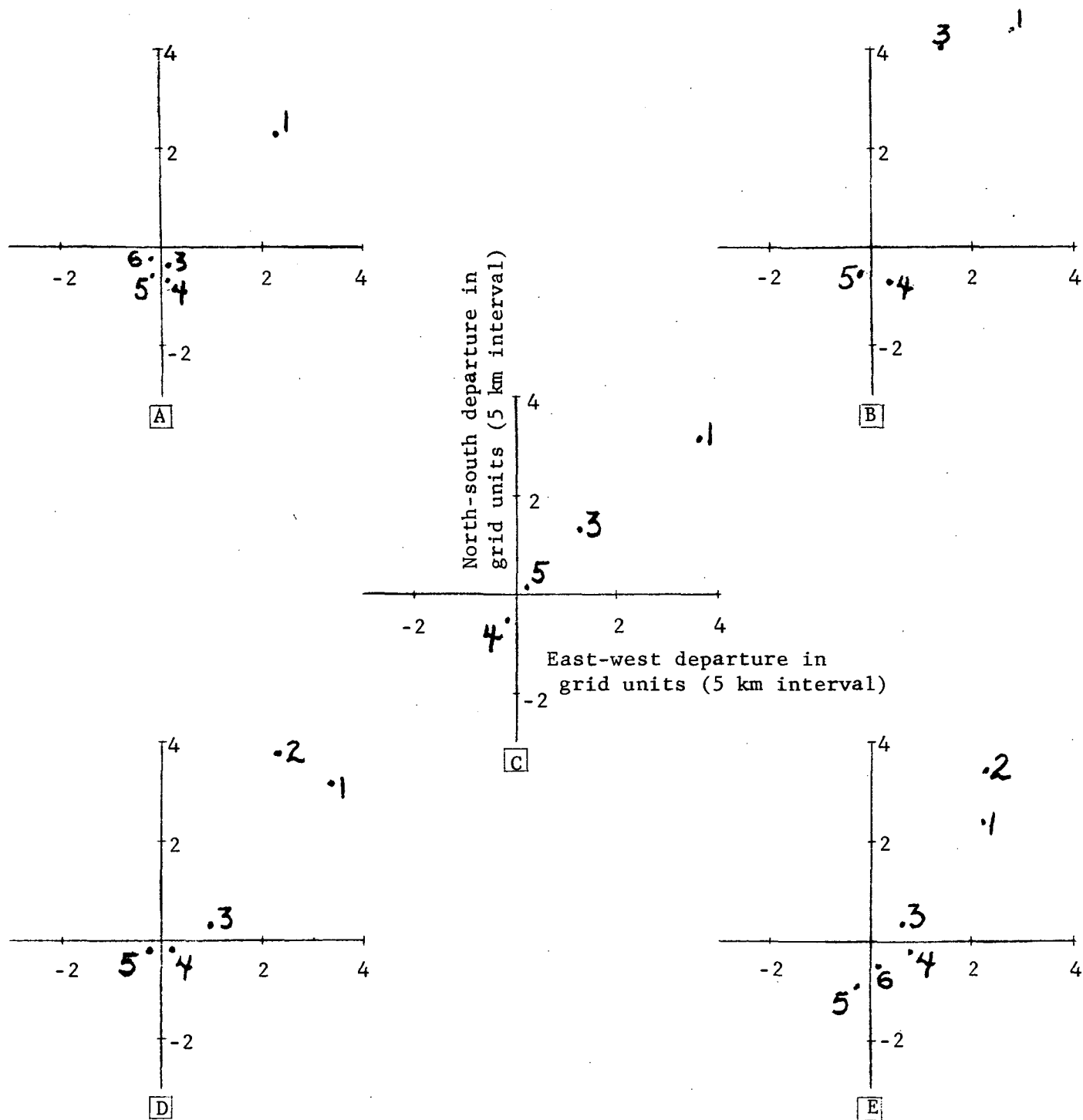


Figure 18. Departures of inner trajectory end points from reference values (using all available data) for Day 197 as the amount of data used in the analysis is varied. Numbers refer to the data set of Table 1 employed in each analysis. Low numbers not shown are off-scale. High numbers not shown are essentially equal to the reference value.

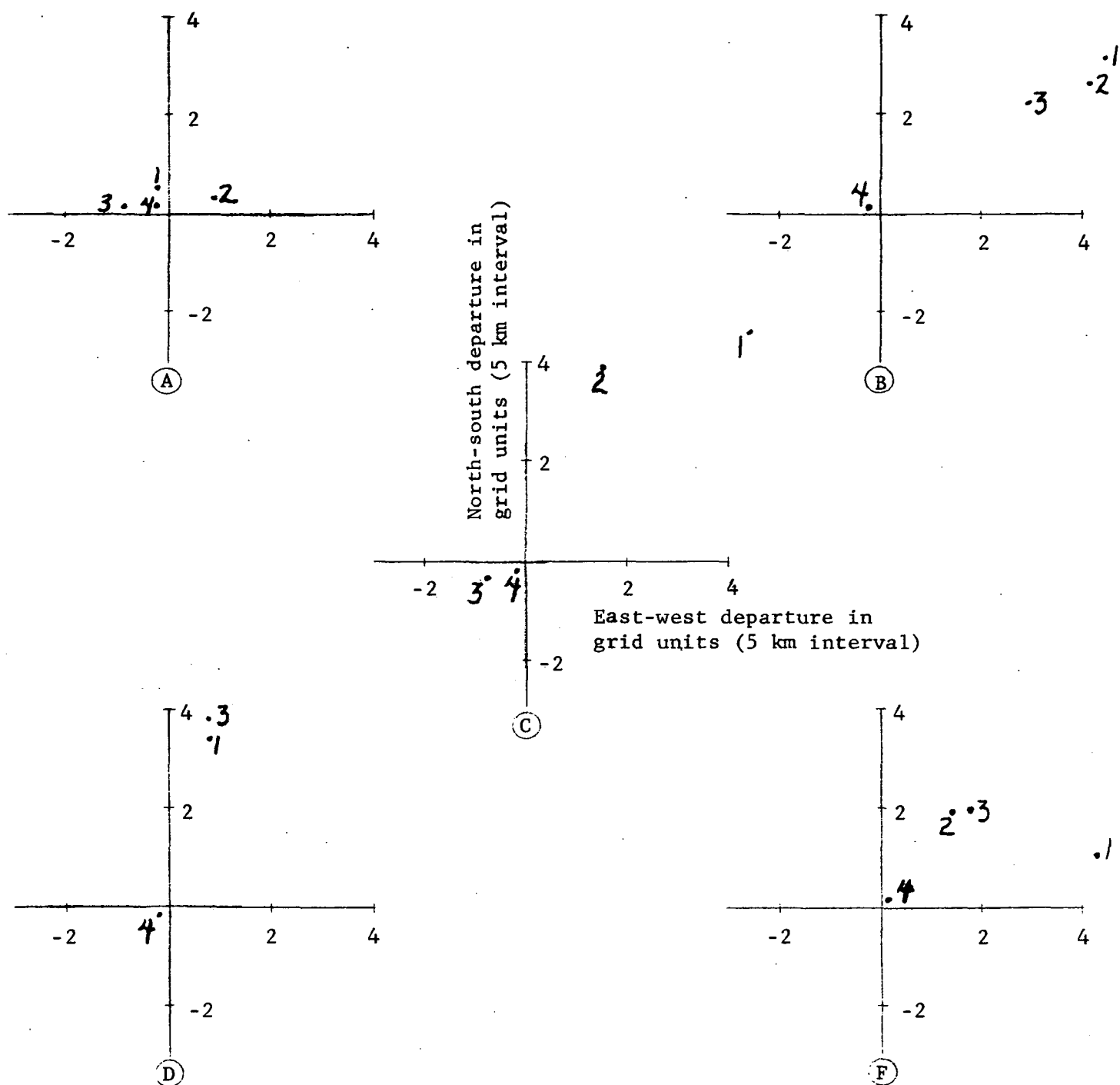


Figure 19. Departures of outer trajectory end points from reference values (using all available data) for Day 197 as the amount of data used in the analysis is varied. Numbers refer to the data set of Table 1 employed in each analysis. Low numbers not shown are off-scale. High numbers not shown are essentially equal to the reference value.

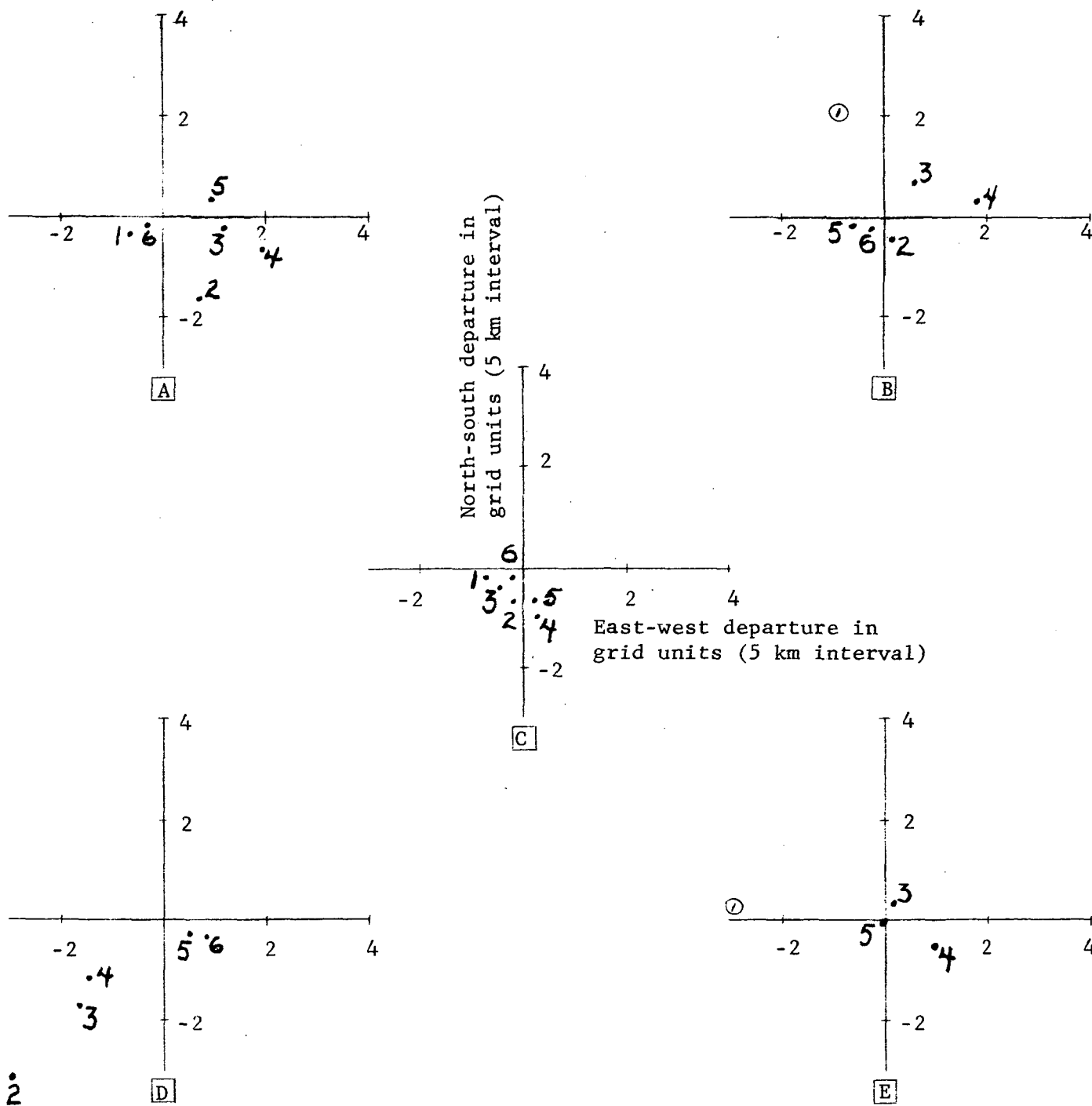


Figure 20. Departures of inner trajectory end points from reference values (using all available data) for Day 210 as the amount of data used in the analysis is varied. Numbers refer to the data set of Table 1 employed in each analysis. Low numbers not shown are off-scale. High numbers not shown are essentially equal to the reference value.

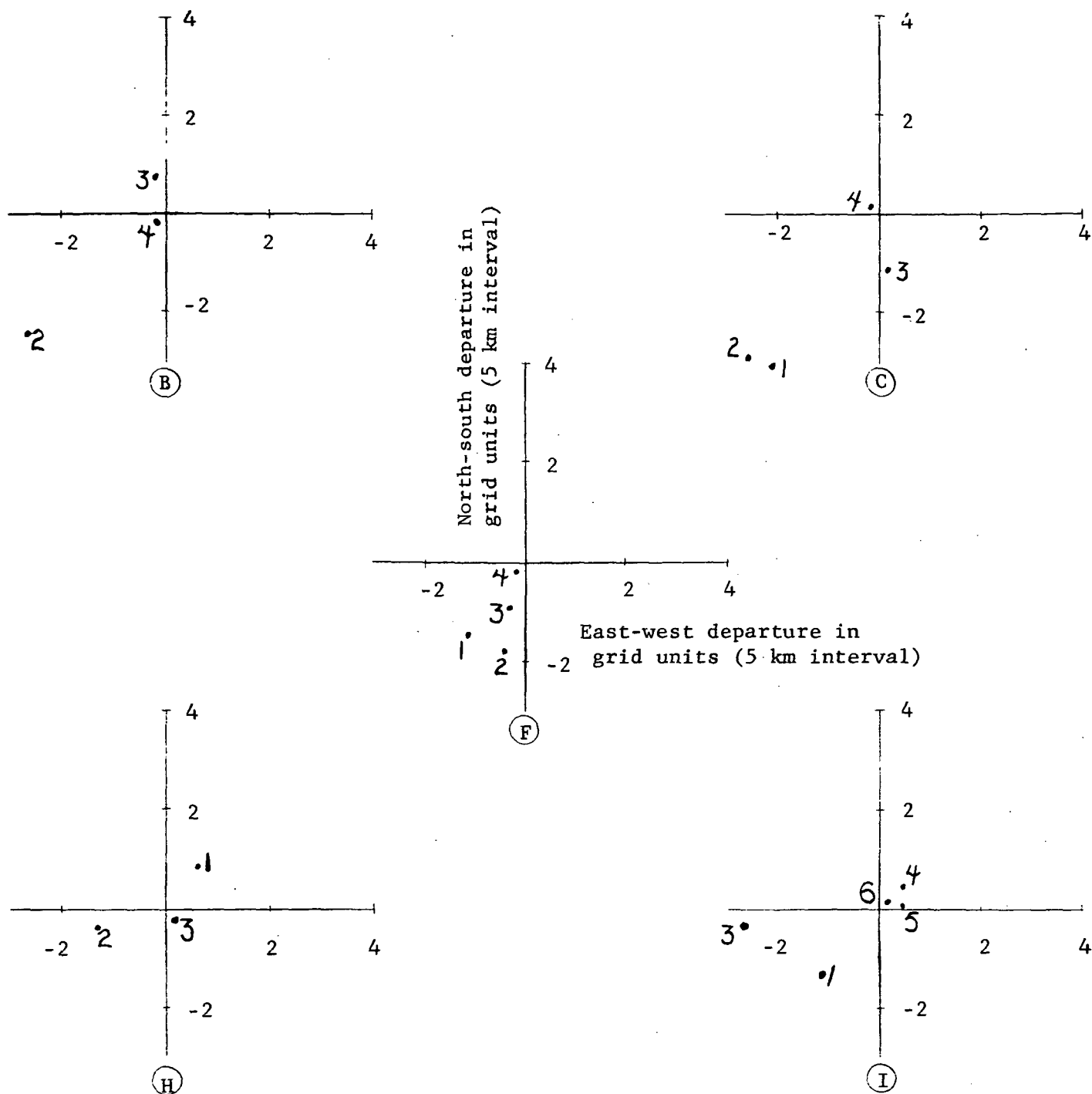


Figure 21. Departures of outer trajectory end points from reference values (using all available data) for Day 210 as the amount of data used in the analysis is varied. Numbers refer to the data set of Table 1 employed in each analysis. Low numbers not shown are off-scale. High numbers not shown are essentially equal to the reference value.

The outer trajectory end point differences for the two days are plotted in Figures 19 and 21, respectively. The outer trajectory end points are seen to converge somewhat more rapidly to their final values than the inner trajectory end points do. The reason for this is that the objective analysis is accomplished in such a way that the variability of the wind field from the dense inner network does not propagate into the outer regions. Therefore, adding more data from the interior stations does little to affect trajectories which do not pass through the interior region. The inner trajectories converge more slowly to their final values because the data which are added to higher numbered data sets contain information from the innermost stations which will refine the analyzed wind field in the inner region.

A slightly different approach is to investigate the sensitivity of computed trajectories to the effect of dropping observations from selected individual stations. An error, ϵ , is defined as the distance between end points of two trajectories originating from the same starting point; one trajectory is computed from complete data and the second is computed from the same data base less one station. The error, ϵ , should be inversely proportional to the distance, Δ , of closest approach of the second trajectory to the location of the station with missing data. A plot of ϵ versus Δ will reveal the significance of missing data in various portions of the observational network. Observations are dropped individually from the following sequence of stations: 105, 108, 121, and 125. This sequence proceeds from the dense parts of the observing network to the sparse areas. The results of this analysis are presented in Figure 22 (Day 197) and Figure 23 (Day 210). Inspection of these figures reveals that the errors are generally less than one grid interval (5 km) except in the case where data from an outer station (121 or 125) is missing. In fact for the two five-hour periods, there is only one case where dropping the data from an inner station leads to an error in the trajectory end point which is greater than one half grid unit. Figure 23 shows that, on Day 210 when the data from Station 125 is dropped from the analysis, most trajectories depart significantly from their reference values. This would appear to represent an extreme case since on Day 210 data from Stations 112, 119, 120, and 124 are already missing, and dropping data from Station 125 creates an analysis without any observation in a large area to the west and south of the city. This occurrence tends to confirm the importance of certain key

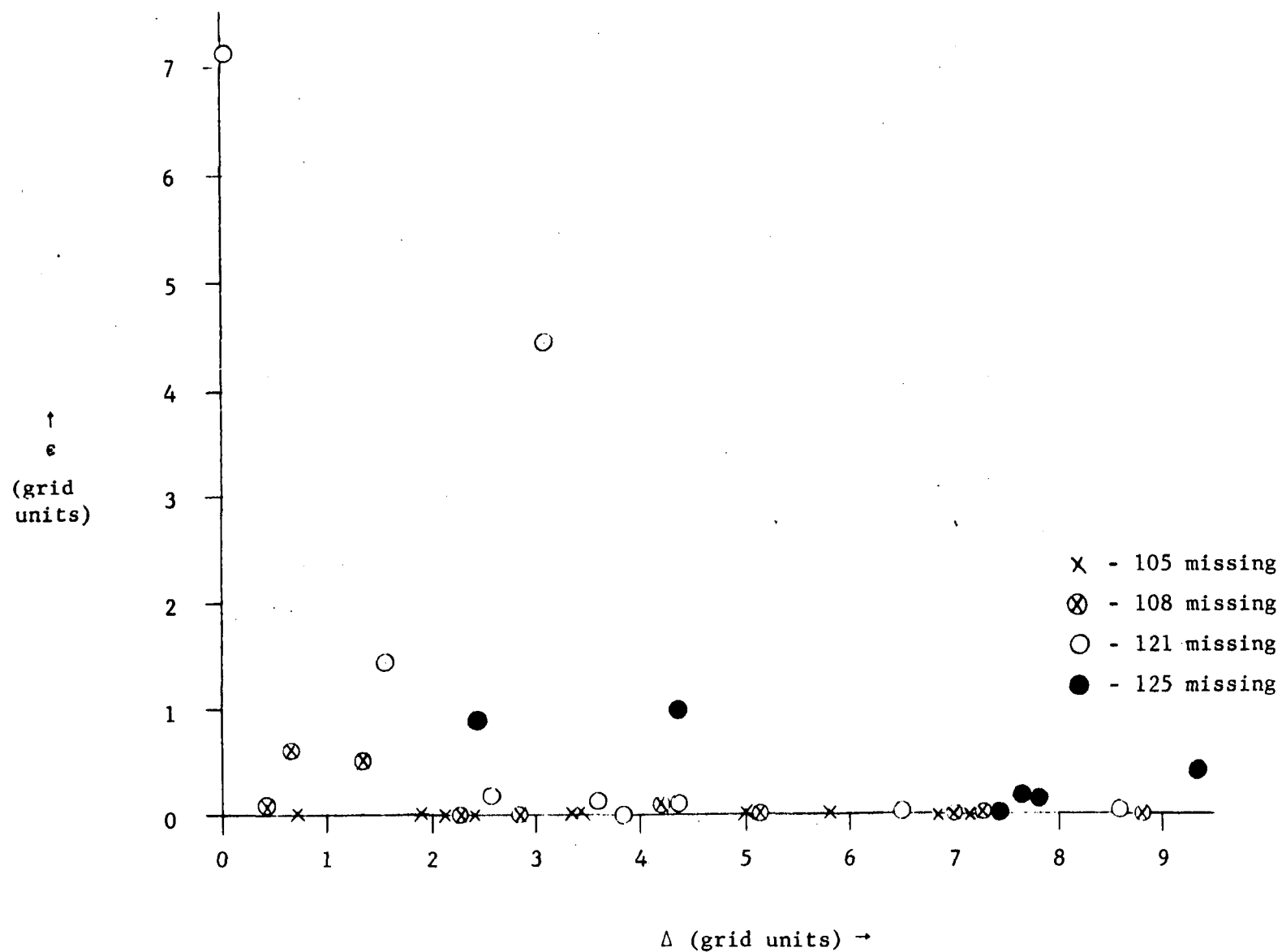


Figure 22. Dependence of the error, ϵ , in trajectory end points with the distance, Δ , of closest approach of the computed trajectory to the missing station for Day 197.

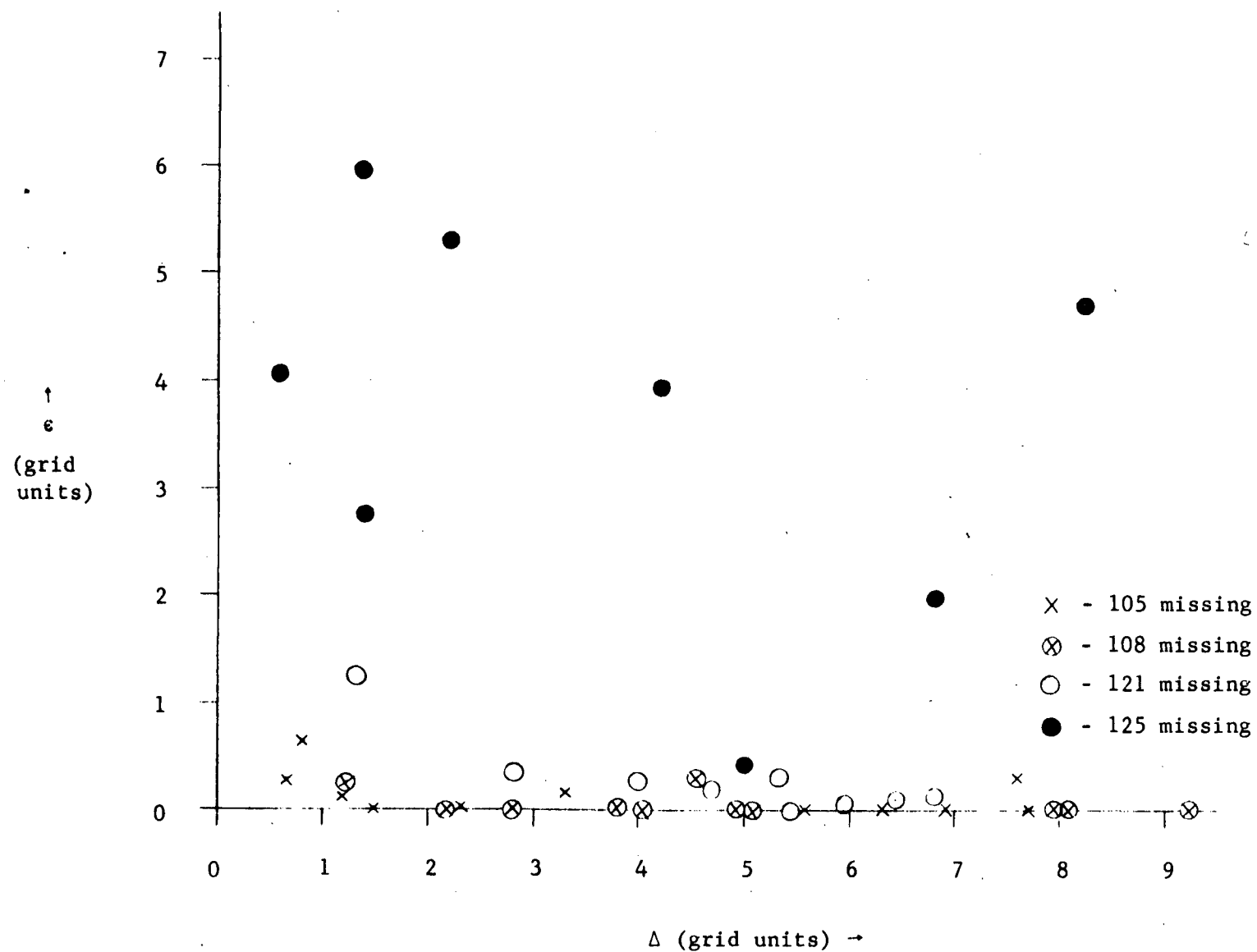


Figure 23. Dependence of the error, ϵ , in trajectory end points with the distance, Δ , of closest approach of the computed trajectory to the missing station for Day 210.

stations in the outermost regions of the network especially when the data from some of the adjacent stations are already missing. With this exception noted, the sensitivity analysis supports the conclusion that the wind field is sufficiently well sampled that computed trajectories are not significantly degraded when data from any single station is lost. The results of the analysis also inspire confidence in the adequacy of the objective analysis routine reported in Part 1 (Hovland, et al., 1976).

REFERENCES

- Hovland, D., D. Dartt and K. Gage: An Objective Analysis Technique for the Regional Air Pollution Study. Final Report, Part 1, Contract No. 68-02-1827 for Environmental Protection Agency, Research Triangle Park, NC, 1976. 52 pp.
- Vukovich, F. M., J. W. Dunn III, and B. W. Crissman: A Theoretical Study of the St. Louis Heat Island: The Wind and Temperature Distribution. J. Appl. Meteor., 15, 417-440, 1976.
- Wendell, L. L.: Mesoscale Wind Fields and Transport Estimates Determined from a Network of Wind Towers. Mon. Wea. Rev., 100, 565-578, 1972.
- Wendell, L. L.: An Evaluation of Data Requirements and Objective Analysis Techniques Appropriate for Regional Scale Atmospheric Transport. Battelle Pacific Northwest Laboratories, BNWL-SA-5234, 1975.

APPENDIX A: PROGRAM LISTINGS

```

SUBROUTINE TRACKS(TRAJX,TRAJY,LEN,M,N,IPT,
1LU,U,V,I,J,K,GRIDSP,NSTEPS,HOURS,NMAPS)
  DIMENSION TRAJX(M,N),TRAJY(M,N),LEN(N),U(I,J,K),V(I,J,K)
C
C  *TRACKS WILL COMPUTE TRAJECTORIES FROM STARTING POINTS GIVEN
C  IN TRAJX(1,L), TRAJY(1,L), L=1,...,N. REMAINING POINTS OF
C  A TRAJECTORY WILL BE IN TRAJX(LL,L), TRAJY(LL,L),
C  LL=2,...,LEN(L). THE LEN(L) WILL BE GENERATED BY TRACKS.
C  IPT WILL GET THE LENGTH OF THE LONGEST TRAJECTORY.
C  *DATA MAPS WILL BE READ INTO COMPONENT ARRAYS U AND V FROM
C  TAPE LU. GRIDSP IS THE DISTANCE BETWEEN GRID POINTS IN KM.
C  NSTEPS IS THE NUMBER OF TIME STEPS BETWEEN MAPS, HOURS IS
C  THE NUMBER OF HOURS BETWEEN MAPS, AND NMAPS IS THE NUMBER
C  OF MAPS TO USE.
C
C  *IPT IS THE INDEX OF THE CURRENT TIME STEP
  I P T = 0
C
  IF(N.LE.0 .OR. I.LE.1 .OR. J.LE.1 .OR. K.LE.1)RETURN
C
C  *CHECK THAT TRAJECTORY ARRAYS ARE LONG ENOUGH
  MAX=NSTEPS*NMAPS+1
  IF(MAX.GT.M)RETURN
C
C  *LEN(L) MAY BE MADE SMALLER LATER
  DO 10 L=1,N
10  LEN(L)=MAX
C
  I P T = 1
C
C  *WIND SPEEDS ARE IN METERS /SEC. CONV CONVERTS
C  TRAJECTORY INCREMENTS TO GRID UNITS.
  CONV=3.6/GRIDSP*HOURS
C
C  *DT IS THE TIME BETWEEN TRAJECTORY STEPS.
  DT=1./NSTEPS
C
C  *READ FIRST MAP.
  READ(LU)((U(II,JJ,1),II=1,I),JJ=1,J),((V(II,JJ,1),II=1,I),JJ=1,J)
C
C  *LOOP THROUGH MAPS
  IMAPS=0
201  IMAPS=IMAPS+1
  IF(IMAPS.GT.NMAPS)GO TO 381
C
C  *READ SECOND MAP.
  READ(LU)((U(II,JJ,2),II=1,I),JJ=1,J),((V(II,JJ,2),II=1,I),JJ=1,J)
C
C  *LOOP FROM ONE MAP TO NEXT
  ISTEPS=0
301  ISTEPS=ISTEPS+1
  IF(ISTEPS.GT.NSTEPS)GO TO 351
C
C  *TIME IS TIME ELAPSED FROM MAP 1
  TIME=(ISTEPS-1.)/NSTEPS

```

```

      IPT=IPT+1
C
C      *LOOP THROUGH TRAJECTORIES.  ICT COUNTS ACTIVE TRAJECTORIES.
      ICT=0
      DO 320 ITR=1,N
C
C      *LENGTH LESS THAN MAX MEANS TRAJECTORY HAS GONE OFF MAP.
      IF(LEN(ITR).LT.MAX)GO TO 320
      ICT=ICT+1
C
C      *FIND X AND Y INCREMENTS AND MOVE TRAJECTORY
      CALL ADVECT(DX,DY,U,V,I,J,K,
1TRAJX(IPT-1,ITR),TRAJY(IPT-1,ITR),TIME,DT,CONV)
      X=TRAJX(IPT-1,ITR)+DX
      TRAJX(IPT,ITR)=X
      Y=TRAJY(IPT-1,ITR)+DY
      TRAJY(IPT,ITR)=Y
C
C      *TERMINATE TRAJECTORY IF IT IS OFF THE MAP
      IF(X.LT.0 .OR. X.GT.I-1)GO TO 315
      IF(0.LE.Y .AND. Y.LE.J-1)GO TO 320
315  LEN(ITR)=IPT
320  CONTINUE
C
C      *RETURN IF ALL TRAJECTORIES ARE OFF THE MAP
      IF(ICT.NE.0)GO TO 301
      IPT=IPT-1
      GO TO 381
C
C      *REPLACE FIRST MAP WITH SECOND MAP.
351  DO 360 JJ=1,J
      DO 360 II=1,I
      U(II,JJ,1)=U(II,JJ,2)
360  V(II,JJ,1)=V(II,JJ,2)
      GO TO 201

381  RETURN
      END

```



```

SUBROUTINE ADVECT(DELX,DELY,U,V,I,J,K,X,Y,T,DELT,CONV)
C   DIMENSION U(I,J,K),V(I,J,K)
C
C   *ADVECT FINDS DELX AND DELY WHICH ARE APPROXIMATIONS TO THE
C   X AND Y DISPLACEMENTS OF AN AIR PARCEL BETWEEN TIME T
C   AND TIME T + DELT
C   *THE WIND FIELDS ARE DEFINED BY THE COMPONENT ARRAYS U AND V.
C   (X,Y,T) IS THE CURRENT POSITION RELATIVE TO (1,1,1).
C   (X,Y,T) AND (X,Y,T+DELT) MUST BE ON THE MAP.
C
C   *CONV IS A CONVERSION FACTOR TO GET DELX AND DELY IN GRID UNITS.
C   CON=CONV*DELT
C
C   *FIRST DISPLACEMENTS ARE BASED ON WIND AT CURRENT POSITION
C   DX1=TRILI(U,I,J,K,X,Y,T)*CON
C   DY1=TRILI(V,I,J,K,X,Y,T)*CON
C
C   *SECOND DISPLACEMENTS ARE BASED ON WIND AT DISPLACED POSITION.
C   DISPLACED POSITION MUST BE ON MAP.
C   XP=X+DX1
C   IF(XP.LT.0 .OR. XP.GT.I-1)GO TO 13
C   YP=Y+DY1
C   IF(0.LE.YP .AND. YP.LE.J-1)GO TO 15
13  XP=X
C   YP=Y
15  TP=T+DELT
C   DX2=TRILI(U,I,J,K,XP,YP,TP)*CON
C   DY2=TRILI(V,I,J,K,XP,YP,TP)*CON
C
C   *FINAL DISPLACEMENTS ARE AVERAGE OF FIRST TWO.
C   N.B. (X+DELX,Y+DELY,T+DELT) MAY BE OFF MAP.
C   DELX=0.5*(DX1+DX2)
C   DELY=0.5*(DY1+DY2)
C
C   RETURN
C   END

```

```

FUNCTION TRILI(A,L,M,N,X,Y,Z)
DIMENSION A(L,M,N)
C
C *A IS AN ARRAY OF DIMENSION (L,M,N) HOLDING 3-DIMENSIONAL GRID
C POINT DATA. TRILI WILL INTERPOLATE A VALUE AT THE INTERNAL
C POINT (X,Y,Z) WHERE X, Y, AND Z ARE MEASURED RELATIVE TO (1,1,1)
C TRILI USES TRILINEAR INTERPOLATION. IT REDUCES TO
C 2-DIMENSIONAL BILINEAR INTERPOLATION WHENEVER Z IS AN INTEGER.
C
C *FIND INDEXES OF NEAREST GRID POINT IN THE DIRECTION OF (1,1,1)
C AND THE P, Q AND R DISTANCES FROM THAT GRID POINT.
I=X+1.
P=X-(I-1)
J=Y+1.
Q=Y-(J-1)
K=Z+1.
R=Z-(K-1)

TRILI=(1.-R)*(P*(Q*A(I+1,J+1,K)+(1.-Q)*A(I+1,J,K))
1      +(1.-P)*(Q*A(I,J+1,K)+(1.-Q)*A(I,J,K)))
C
C *R IS 0 IF K IS AN INTEGER
C IF(R.EQ.0)RETURN

TRILI=TPILI+R*(P*(Q*A(I+1,J+1,K+1)+(1.-Q)*A(I+1,J,K+1))
1      +(1.-P)*(Q*A(I,J+1,K+1)+(1.-Q)*A(I,J,K+1)))

RETURN
END

```

APPENDIX B: PROGRAM DOCUMENTATION

SUBROUTINE TRACKS will compute horizontal trajectories from a time sequence of gridded wind fields. The wind fields are stored in component form: u is the west-east component in meters/sec, and v is the south-north component in meters/sec.

The wind fields must be written one per record on a file such that they can be read with the statement

```
READ(LU)((U(II,JJ,1),II=1,I),JJ=1,J),((V(II,JJ,1),II=1,I),JJ=1,J)
```

where LU, I, and J are explained below. Grid point (1,1) is in the south-west corner. I increases to the east, and J increases to the north.

To compute backward trajectories the wind fields must be stored in reverse chronological order. In addition, the components must be replaced by their negatives.

The following elements are parameters to SUBROUTINE TRACKS:

<u>Element</u>	<u>Input or Output</u>	<u>Explanation</u>
TRAJX(M,N) & TRAJY(M,N)	Input & Output	Arrays which will contain the u and v coordinates of the N trajectories to be computed. M must be at least as large as the number of points in the longest trajectory. TRAJX and TRAJY are measured in grid units relative to grid point (1,1). Starting points must be supplied in TRAJX(1,L),TRAJY(1,L), $L=1, \dots, N$.
LEN(N)	Output	Array which will hold the lengths (number of points) of the N trajectories.

(Continued)

<u>Element</u>	<u>Input or Output</u>	<u>Explanation</u>
M,N	Input	Dimensions of arrays TRAJX and TRAJY (and LEN). N is also the number of trajectories to be generated (at least 1).
IPT	Output	Length of the longest trajectory generated, i.e., IPT is the largest of the LEN(L).
LU	Input	Tape number of the file on which the wind fields are stored.
U,V	-	Component arrays into which the gridded wind fields are read. Together U and V are referred to as a map.
I,J,K	Input	Dimensions of U and V. I,J,K must each be greater than 1. K need be no greater than 2.
GRIDSP	Input	Distance (in km) between grid points.
NSTEPS	Input	Number of time steps to use between maps.
HOURS	Input	Number of hours between map times.
NMAPS	Input	Number of maps to use. The first map is map 0; therefore, NMAPS+1 maps must be provided on TAPE LU.

APPENDIX C: USER GUIDE TO ARCHIVE TAPES

The surface and upper air analyses are on seven reels of BCD tape written in even parity at 556 BPI.

	<u>Reel</u>	<u>Dates</u>	<u>No. of Blocks</u>
Surface	1	7/14-8/15, 1975	1584
Upper Air	1	7/14-7/19, 1975	3465
Upper Air	2	7/20-7/25, 1975	3420
Upper Air	3	7/26-7/31, 1975	3455
Upper Air	4	8/01-8/06, 1975	2991
Upper Air	5	8/07-8/11, 1975	2880
Upper Air	6	8/12-8/15, 1975	2309

On each reel the data blocks are followed by a double end-of-file.

The surface analyses are based on observations from Stations 101-125.

The upper air analyses are based on pibal observations from Stations 141-144.

Station coordinates are given in grid units (5 km. spacing). Point (1.00, 1.00) is in the southwest corner of the grid. The x coordinate increases to the east and the y coordinate increases to the north.

<u>Station No.</u>	<u>x Coordinate</u>	<u>y Coordinate</u>
101	11.00	11.00
102	10.67	12.24
103	11.68	11.52
104	11.63	10.49
105	10.90	10.32
106	9.90	10.54
107	10.20	11.55
108	11.84	13.25
109	13.32	11.00
110	11.61	9.59
111	9.93	9.52
112	8.95	11.21
113	9.71	12.99
114	11.03	14.52
115	13.59	14.59
116	14.72	13.04
117	14.28	9.59
118	10.78	7.68
119	8.12	9.14
120	6.78	12.21
121	8.65	15.50
122	10.49	20.87
123	17.63	12.30
124	12.02	2.34
125	1.65	11.48
141	10.75	10.84
142	5.30	8.25
143	14.22	6.44
144	13.34	16.64

ARCHIVE FORMAT FOR SURFACE WIND ANALYSES

<u>FIELD</u>	<u>FORMAT</u>	<u>CONTENTS</u>
1	I2	Year (75)
2	I3	Day (1-365)
3	I2	Hour (0-23)
4	A13	^SURFACE^WIND (BCD Characters)
5-54	25(2F4.1)	Direction (degrees) and speed (mps) for Stations 101-125. 999.0 (9990) represents missing.
55-936	441(2F4.1)	Analyzed data: direction (degrees) and speed (mps) for 441 grid points. 999.0 (9990) represents missing.
937	2X	Blank fill

Total block length is 3750 characters. Each block contains the surface wind analysis for one observation time.

The analysis grid has $2 \times 21 \times 21 = 882$ points:
 $((DIR(I,J),SPD(I,J),I=1,21),J=1,21)$. Grid point (1,1) is in the southwest corner. I increases to the east, and J increases to the north.

Each surface wind analysis is followed by a surface temperature analysis for the same hour.

ARCHIVE FORMAT FOR SURFACE TEMPERATURE ANALYSES

<u>FIELD</u>	<u>FORMAT</u>	<u>CONTENTS</u>
1	I2	Year (75)
2	I3	Day (1-365)
3	I2	Hour (0-23)
4	A13	^SURFACE^TEMP (BCD Characters)
5-29	25F4.1	Temperature (C) for Stations 101-125. 999.0 (9990) represents missing.
30-470	441F4.1	Analyzed data: temperature (C) for 441 grid points. 999.0 (9990) represents missing.
471	16X	Blank fill

Total block length is 1900 characters. Each block contains the surface temperature analysis for one observation time.

The analysis grid has $21 \times 21 = 441$ points:
 ((TEMP(I,J),I=1,21),J=1,21). Grid point (1,1) is in the southwest corner.
 I increases to the east, and J increases to the north.

Each surface temperature analysis is preceded by a surface wind analysis for the same hour.

ARCHIVE FORMAT FOR UPPER AIR WIND ANALYSES

<u>FIELD</u>	<u>FORMAT</u>	<u>CONTENTS</u>
1	I4	Year (1975)
2	I2	Month (1-12)
3	I2	Day (1-31)
4	I2	Hour (0-23)
5	I4	Level, meters above mean sea level.
6	A6	M _A WIND (BCD Characters)
7-14	4(2F5.1)	Direction (degrees) and speed (mps) for Stations 141-144. 999.0 (^9990) represents missing.
15-896	441(2F4.1)	Analyzed data: direction (degrees) and speed (mps) for 441 grid points. 999.0 (9990) represents missing.
897	12X	Blank fill

Total block length is 3600 characters. Each block contains the analysis for one level, at one observation time. Only those levels for which at least one station has data are included on the tape.

The analysis grid has $2 \times 21 \times 21 = 882$ points:
 $((DIR(I,J),SPD(I,J),I=1,21),J=1,21)$. Grid point (1,1) is in the southwest corner. I increases to the east, and J increases to the north.

TECHNICAL REPORT DATA <i>(Please read instructions on the reverse before completing)</i>		
1. REPORT NO. EPA-600/4-77-002b	2.	3. RECIPIENT'S ACCESSION NO.
4. TITLE AND SUBTITLE AN OBJECTIVE ANALYSIS TECHNIQUE FOR THE REGIONAL AIR POLLUTION STUDY Part II	5. REPORT DATE February 1977	6. PERFORMING ORGANIZATION CODE
7. AUTHOR(S) D. Hovland, D. Dartt, and K. Gage	8. PERFORMING ORGANIZATION REPORT NO.	
9. PERFORMING ORGANIZATION NAME AND ADDRESS Control Data Corporation 8100 South 34th Ave. Minneapolis, MN 55440	10. PROGRAM ELEMENT NO. 1AA603	11. CONTRACT/GRANT NO. 68-02-1827
12. SPONSORING AGENCY NAME AND ADDRESS Environmental Sciences Research Laboratories Office of Research and Development U.S. Environmental Protection Agency Research Triangle Park, N.C. 27711	13. TYPE OF REPORT AND PERIOD COVERED Final	14. SPONSORING AGENCY CODE EPA-ORD
15. SUPPLEMENTARY NOTES Part I of this report has been issued as EPA-600/4-77-002a, January 1977		
16. ABSTRACT <p>This report discusses the application of objective analysis techniques to the computation of trajectories from surface wind observations of the Regional Air Pollution Study in St. Louis. Trajectories were computed over a 100-kilometer square grid centered on St. Louis for two 5-hour periods during July 1975. The variability of the surface wind field was investigated by examining the temporal and spatial variability of computed trajectories. Also, the sensitivity of the computed trajectories to the amount of data employed in the analysis was examined in some detail. The results showed a general lack of sensitivity of the computed trajectories to a single missing observation. However, computed trajectories were very sensitive to missing adjacent observations.</p> <p>In addition to the trajectory analysis, a set of tapes containing gridded winds and temperatures for the St. Louis area were generated.</p>		
17. KEY WORDS AND DOCUMENT ANALYSIS		
a. DESCRIPTORS	b. IDENTIFIERS/OPEN ENDED TERMS	c. COSATI Field/Group
*Air Pollution *Meteorological data *Wind (meteorology) *Temperature *Grids (coordinates) *Atmospheric models *Applications of mathematics	St. Louis, Mo.	13B 04B 08B 04A 12A
18. DISTRIBUTION STATEMENT RELEASE TO PUBLIC	19. SECURITY CLASS (This Report) UNCLASSIFIED	21. NO. OF PAGES 57
	20. SECURITY CLASS (This page) UNCLASSIFIED	22. PRICE